

RECLAMATION

Managing Water in the West

Evaluation of Land Subsidence Impacts Due to Groundwater Pumping Near the Delta-Mendota Canal

**Research and Development Office
Science and Technology Program
(Final Report) ST-2017-3117-01**



**U.S. Department of the Interior
Bureau of Reclamation
Research and Development Office**

October 2017

Mission Statements

Protecting America's Great Outdoors and Powering Our Future

The Department of the Interior protects and manages the Nation's natural resources and cultural heritage; provides scientific and other information about those resources; and honors its trust responsibilities or special commitments to American Indians, Alaska Natives, and affiliated island communities.

Disclaimer:

This document has been reviewed under the Research and Development Office Discretionary peer review process https://www.usbr.gov/research/peer_review.pdf consistent with Reclamation's Peer Review Policy CMP P14. It does not represent and should not be construed to represent Reclamation's determination, concurrence, or policy.

REPORT DOCUMENTATION PAGE		<i>Form Approved</i> <i>OMB No. 0704-0188</i>	
T1. REPORT DATE: OCTOBER 2017	T2. REPORT TYPE: RESEARCH	T3. DATES COVERED 10/01/14 to 09/30/17	
T4. EVALUATION OF LAND SUBSIDENCE IMPACTS DUE TO GROUNDWATER PUMPING NEAR THE DELTA-MENDOTA CANAL		5a. CONTRACT NUMBER RY154RD201523117	
		5b. GRANT NUMBER	
		5c. PROGRAM ELEMENT NUMBER 1541 (S&T)	
6. AUTHOR(S) Kirk Nelson Bureau of Reclamation 2800 Cottage Way Sacramento, CA 95825		5d. PROJECT NUMBER ST-2017-3017-01	
		5e. TASK NUMBER	
		5f. WORK UNIT NUMBER MP-740	
7. PERFORMING ORGANIZATION NAME(S) AND ADDRESS(ES) Kirk Nelson Bureau of Reclamation 2800 Cottage Way Sacramento, CA 95825		8. PERFORMING ORGANIZATION REPORT NUMBER	
9. SPONSORING / MONITORING AGENCY NAME(S) AND ADDRESS(ES) Research and Development Office U.S. Department of the Interior, Bureau of Reclamation, PO Box 25007, Denver CO 80225-0007		10. SPONSOR/MONITOR'S ACRONYM(S) R&D: Research and Development Office BOR/USBR: Bureau of Reclamation DOI: Department of the Interior	
		11. SPONSOR/MONITOR'S REPORT NUMBER(S) ST-2017-3117-01	
12. DISTRIBUTION / AVAILABILITY STATEMENT Final report can be downloaded from Reclamation's website: https://www.usbr.gov/research/			
13. SUPPLEMENTARY NOTES			
14. ABSTRACT <i>This project developed and applied a groundwater model of the San Joaquin Valley to assess the relationship between groundwater pumping and land subsidence. The intent is to aid water managers in decision making aimed at mitigating the subsidence risk, particularly near the Delta-Mendota Canal. Towards this aim, the HydroGeoSphere San Joaquin Valley Model (HGSSJVM) was developed and applied to gain a better understanding of the factors governing the groundwater/land subsidence relationship. An initial version of the model was built and calibrated for a simulation period of April 1961 through September 2003; this was extended to September 2013. A preliminary analysis using the extended HGSSJVM suggests that the location of the wells used and pumping magnitude are important. The timing factor was found to be relatively unimportant, but subsidence impacts may be mitigated by distributing a given volume of pumping for an irrigation season over a longer period of time.</i>			
15. SUBJECT TERMS Land subsidence, groundwater, models			
16. SECURITY CLASSIFICATION OF:	17. LIMITATION OF ABSTRACT U	18. NUMBER OF PAGES	19a. NAME OF RESPONSIBLE PERSON Kirk Nelson

a. REPORT U	b. ABSTRACT U	c. THIS PAGE U		56	19b. TELEPHONE NUMBER 916-978-5066
-----------------------	-------------------------	--------------------------	--	----	--

S Standard Form 298 (Rev. 8/98)
P Prescribed by ANSI Std. Z39-18

BUREAU OF RECLAMATION

Research and Development Office
Science and Technology Program

Mid-Pacific Region, 86-68

(Final Report) ST-2017-3117-01

Evaluation of Land Subsidence Impacts Due to Groundwater Pumping Near the Delta-Mendota Canal



Prepared by: **Kirk Nelson**
Civil Engineer, Mid-Pacific Region, 86-68



Peer Review: **Nigel Quinn, P.E.**
Water Resources System Engineer, 86-68

For Reclamation disseminated reports, a disclaimer is required for final reports and other research products, this language can be found in the peer review policy:

This document has been reviewed under the Research and Development Office Discretionary peer review process https://www.usbr.gov/research/peer_review.pdf consistent with Reclamation's Peer Review Policy CMP P14. It does not represent and should not be construed to represent Reclamation's determination, concurrence, or policy.

Acknowledgements

Technical guidance was provided by René Therrien (Université Laval) regarding use of the HydroGeoSphere code including the subsidence module. Tom Heinzer (Reclamation, Mid-Pacific Region, GIS group) was instrumental in development of the HGSSJVM model grid. George Matanga (Reclamation, Mid-Pacific Region, Division of Planning) assisted with conceptual model development. Lisa Rainger (Reclamation, Mid-Pacific Region, Division of Planning) assisted with data visualization. Clarence Leung (Reclamation, Mid-Pacific Region, Division of Planning) provided additional GIS support. Computing resources were provided by the Lawrence Berkeley National Laboratory's (LBNL) National Energy Research Scientific Computing Center (NERSC).

Acronyms and Abbreviations

BC	Boundary condition
CVHM	Central Valley Hydrologic Model
CVHM2	Central Valley Hydrologic Model-2
CVP	Central Valley Project
DWR	California Department of Water Resources
DMC	Delta-Mendota Canal
ET	Evapotranspiration
FMP	Farm Process package
GSA	Groundwater Sustainability Agency
HGS	HydroGeoSphere
HGSSJVM	HydroGeoSphere San Joaquin Valley Model
PEST	Model-independent Parameter Estimation software
RMSD	Root mean square deviation
SGMA	Sustainable Groundwater Management Act
SENSAN	Sensitivity analyzer of PEST
SJV	San Joaquin Valley
USGS	United States Geological Survey

Executive Summary

The San Joaquin Valley (SJV) of California is among the more notable areas of the world to have experienced significant land subsidence impacts due to groundwater pumping. The development of the SJV into a major agricultural producing region in the 20th Century was associated initially with a reliance on groundwater pumping as the primary source of irrigation water. Groundwater pumping rates grew far beyond what the underlying aquifer could sustain, and one of the negative impacts of this overreliance on groundwater was dramatic land subsidence, affecting 5200 mi² of irrigable land (one-half of the entire valley) with a maximum subsidence level of 29.6 ft recorded in western Fresno County in 1977 (Ireland et al., 1984). The Central Valley Project (CVP) was constructed by the Bureau of Reclamation in large part to address the negative impacts (including land subsidence) of the groundwater overdraft that was being caused by the expansion of irrigated agriculture in the SJV. In the 1960's, the imported surface water of the CVP started to reduce the need for accessing groundwater as a source of irrigation water and, thus, slow down and in some case halt the processes of subsidence that were occurring throughout the SJV. However, periods of drought (e.g., 1976-1977, 1986-1992, 2007-2009, 2011-2015), coupled with a recognition of the need to balance the multiple uses of CVP water (e.g., ecological benefits, flood control, urban and agricultural demands), have limited the degree to which imported CVP surface water can offset the incentive for irrigators to tap into dwindling groundwater supplies. As a result, groundwater overdraft is still occurring (particularly in years experiencing drought conditions), and land subsidence has continued to occur (Sneed et al., 2013). Land subsidence is of particular concern to Reclamation because of the direct impacts to the Delta-Mendota Canal (DMC), Reclamation's primary conveyance facility for CVP water in the SJV. Land subsidence has caused damage to the canal, including buckling, reversal of hydraulic gradients, and reduction of delivery capacity. Reclamation does not have management oversight of most groundwater pumping in the SJV. However, Reclamation does play a role in the Warren Act program which allows well owners to pump groundwater into the DMC for delivery to downstream users in dry years.

In consideration of the problems described above, this project was undertaken to develop and apply a groundwater model of the SJV with the objective of providing an analytical tool capable of assessing the relationship between groundwater pumping and land subsidence that could aid water managers in decision making aimed at mitigating the subsidence risk, with a particular focus on the area around the DMC in the western SJV. Towards this aim, the HydroGeoSphere San Joaquin Valley Model (HGSSJVM) was developed and applied by the research project described herein to gain a better understanding of the factors governing the groundwater / land subsidence relationship to assist decision makers in better managing the land subsidence risk.

This research built upon earlier work performed by the MP region in developing the HGSSJVM. Basic model construction of HGSSJVM (e.g., model grid development, initial and boundary condition specifications, construction of time series defining model stresses) had been completed prior to the beginning of this research. In the first year (FY 2015) of this three-year research project, two objectives were accomplished: 1) calibration to historical groundwater levels and subsidence measurements for the period of April 1961 through September 2003; 2) a preliminary analysis of the relative importance of groundwater pumping magnitude, timing of the groundwater withdrawals, and location along the DMC of the wells used in the Warren Act pumping program, using the calibrated model, in a set of 27 model scenarios compared against the baseline historical

model. The results of the preliminary analysis suggested that timing of the groundwater withdrawals had a negligible impact on subsidence, location of the wells used had a small impact, and the overall magnitude of the Warren Act pumping had the greatest impact.

Year two of the project (FY 2016) focused on extending the model simulation period through the 2013 water year. This model extension allows HGSSJVM to account for some of the more recently observed significant measurements of subsidence. Appropriate groundwater level and subsidence measurement data were added to the HGSSJVM calibration dataset for the newly added model simulation period (October 2003 through September 2013), and the HGSSJVM model parameters were recalibrated for the entire new model simulation parameter (April 1961 through September 2013) using the original model calibration dataset augmented by the additional calibration data assembled.

Year three of the project (FY 2017) used the extended HGSSJVM in a comprehensive sensitivity analysis examining the relationship between groundwater pumping and land subsidence in the western SJV. Four factors were considered: 1) groundwater pumping magnitude; 2) timing of the groundwater withdrawals; 3) location along the DMC of the wells used in the Warren Act pumping program; 4) number of months (duration) over which the Warren Act pumping was distributed. The results of this sensitivity analysis suggest that the location of the wells used was the most important factor, followed by the magnitude of pumping. The timing factor was found to be relatively unimportant in governing the groundwater / land subsidence relationship, but the duration factor was found to have a small beneficial impact in reducing subsidence when the given volume of pumping for an irrigation season was distributed over a longer period of months.

Contents

Executive Summary	viii
Main Report	1
Conclusion & Next Steps.....	54
References.....	55

Tables

Table 1. Aquifer properties transferred from CVHM to HGSSJVM for steady-state model.	5
Table 2. Final calibrated values of infiltration and exfiltration (positive values indicate infiltration; negative values indicate exfiltration).....	8
Table 3. Calibration parameter values following manual calibration.....	16
Table 4. Calibration parameter values following PEST calibration.	16
Table 5. Preliminary Analysis Model Scenarios.....	23
Table 6. Calibration parameter values for original HGSSJVM (1961-2003).....	34
Table 7. Calibration parameter values for extended HGSSJVM (1961-2013).....	34
Table 8. Warren Act Wells	38
Table 9. Water Year Types	39
Table 10. Sensitivity Scenarios.....	40
Table 11. Simulation Observation Wells.....	43
Table 12. Mean slope of sensitivity for each sensitivity parameter.....	54
Table 13. Summary of Sensitivity Analysis Results.....	54
Table 14. Differential Subsidence Locations.....	55

Figures

Figure 1. HGSSJVM model grid. Blue nodes = boundary with a constant head BC (0 m).	7
Figure 2. Refinement of HGSSJVM Grid near the Delta-Mendota Canal.	9
Figure 3. Contour plot comparing observed water table elevations versus HGSSJVM simulated water table elevations.	10
Figure 4. Scatter plot comparing observed water table elevations versus HGSSJVM simulated water table elevations.	11
Figure 5. Distribution of groundwater well locations in HGSSJVM.	14
Figure 6. Measured and simulated subsidence at locations near the Delta-Mendota Canal.	21
Figure 7. Preliminary Analysis Model Scenario Results. Simulated subsidence for the 27 scenarios compared with the baseline model at the seven subsidence locations along the DMC.	30
Figure 8. Increased Subsidence from 10% Increase in Background Pumping	31
Figure 9. Observed versus simulated subsidence values at Oro Loma	35
Figure 10. Warren Act Wells and Simulation “Observation” Wells	44
Figure 11. Groundwater Levels at Oro Loma versus Pumping Magnitude. Simulated groundwater levels at the end of the simulation period	46
Figure 12. Subsidence values at Oro Loma versus Pumping Magnitude	47
Figure 13. Groundwater Levels at Oro Loma versus Pumping Location	48
Figure 14. Subsidence values at Oro Loma versus Pumping Location	49
Figure 15. Groundwater Levels at Oro Loma versus Pumping Timing	50
Figure 16. Subsidence values at Oro Loma versus Pumping Timing	51
Figure 17. Groundwater Levels at Oro Loma versus Pumping Duration	52
Figure 18. Subsidence values at Oro Loma versus Pumping Duration	53
Figure 19. Differential Subsidence Locations	56

Main Report

Introduction & Background

Land Subsidence/Groundwater Pumping Relationship

There are four types of subsidence occurring in the San Joaquin Valley: (1) subsidence caused by groundwater overdraft and the associated water-level declines; (2) subsidence related to the hydrocompaction of moisture-deficient deposits above the water table; (3) subsidence related to fluid withdrawal from oil and gas fields; (4) subsidence caused by deep-seated tectonic movements; of these groundwater overdraft caused by pumping is the leading cause (Ireland et al., 1984). Thus, understanding and being able to model the land subsidence/groundwater pumping relationship is of prime importance in managing the land subsidence risk, especially in the context of water management decisions in the San Joaquin Valley.

Analytical Tools for Assessing Land Subsidence/Groundwater Pumping in the San Joaquin Valley

The most recent and relevant analytical tool available for assessing the land subsidence/groundwater pumping relationship in the San Joaquin Valley is the Central Valley Hydrologic Model (CVHM) developed by the USGS (Faunt, 2009). CVHM is a regional scale hydrologic model covering the entire Central Valley of California (both Sacramento and San Joaquin Valleys); it is intended to represent the hydrology of the present-day Central Valley which is driven by surface water deliveries and associated groundwater pumping, which in turn reflect spatial and temporal variability in climate, water availability, land use, and the man-made system of water delivery infrastructure (Faunt, 2009). CVHM was constructed using the MODFLOW-2000 (Harbaugh et al., 2000; Hill et al., 2000) finite difference groundwater modeling software with an updated version of the Farm Process package (Schmid et al., 2006). The Farm Process (FMP) package provides a detailed accounting of land use and associated surface water deliveries, groundwater pumping (both specified and computed), and consumptive use. Accordingly, CVHM is able to provide a dynamically integrated water supply-and-demand accounting within agricultural areas and areas of native vegetation. Urban areas are also represented in CVHM based more directly on the available data of water use and groundwater pumping. CVHM accounts for subsidence using the SUB package (Hoffman et al., 2003).

CVHM is a powerful tool for regional hydrologic analyses, but its uniform square mile model grid discretization is not fine enough for detailed assessments of the subsidence risks along structures such as the DMC. A more refined version of CVHM for such purposes is under development but is not yet publicly released; also under development is a new version of CVHM that extends the existing time series by 10 years through water year 2013. The forthcoming new version of CVHM (CVHM2) is expected to have $\frac{1}{4}$ mile constant grid spacing. Thus, no publicly available model with variable grid resolution for examining subsidence impacts on structures such as the DMC currently exists. With this in mind, the original public release of CVHM (Faunt, 2009) was used as the primary basis for development of the HydroGeoSphere San Joaquin Valley Model (HGSSJVM). HGSSJVM was constructed using the HydroGeoSphere model code (Therrien et

al., 2006). Unlike CVHM, HGSSJVM uses variable grid spacing with finer resolution along major features such as the San Joaquin River and the DMC (Figure 2).

Literature Review

The first major study of land subsidence in the SJV was conducted by Poland et al. (1975) who documented the widespread subsidence due to groundwater overdraft that started in the mid-1920's and continued largely unabated until about 1970. The findings of this study included: groundwater withdrawals for irrigation increased from 3 million acre-feet in 1942 to 10 million acre-feet in 1966; groundwater levels declined at unprecedented rates during the 1950's and early 1960's; by 1970, 5200 mi² of the SJV had been affected by land subsidence; maximum subsidence exceeded 28 feet; the total volume of subsidence in the SJV totaled 15.6 million acre-feet which is equivalent to one-half the initial storage capacity of Lake Mead; this subsidence was described as "one of the great environmental changes imposed by man". Poland et al. (1975) also found that importation of surface water, beginning with the northwestern and eastern areas of SJV in the 1950's and then the western and southern areas in the late 1960's, had resulted in rising groundwater levels and a stabilization of elevations of the subsiding land surface by 1973. The Poland et al. report contains 10-13 years of measurements of both groundwater level changes and compaction that form the physical basis for the relationship between groundwater withdrawals and land subsidence.

Ireland et al. (1984) identified three major areas of land subsidence in the SJV: 1) the Los Banos-Kettleman City area (which contains the DMC); 2) the Tulare-Wasco area in Tulare County; 3) the Arvin-Maricopa area in Kern County. This report found that subsidence rates in the Los Banos-Kettleman City area had decreased sharply with the importation of surface water through the California Aqueduct in the late 1960's and early 1970's. However, subsidence increased again during the drought of 1976-77. Extensometer measurements recorded compaction of 0.1 to 0.5 ft in 1977, and this was linked to the heavy demand on groundwater during the drought which resulted in artesian head declines that occurred at a rate 10 to 20 times faster than those that had occurred during the first long-term drawdown period ending in the late 1960's. Ireland et al. (1984) recommended continued monitoring of land subsidence in the SJV via extensometers, water-level measurements, and periodic releveling.

The first major groundwater modeling study of the western SJV was conducted by Belitz et al. (1993). The Belitz model, motivated largely by water quality concerns related to selenium in agricultural drain water, was constructed using hydrologic data to represent a simulation period of 1972 to 1988. The model covers 550 mi², including the Panoche Creek alluvial fan and parts of the Little Panoche Creek and Cantua Creek alluvial fans; this modeled area includes the southern portion of the DMC. Larson et al. (2001) used a modified version of the Belitz model to simulate land subsidence in the Los Banos-Kettleman City area in order to generate estimates of safe groundwater yields that would avoid significant inelastic subsidence and could be achieved under different management scenarios. Larson et al. used the Interbed Storage Package-1 (IBS1) (Leake and Prudic, 1991) of MODFLOW (McDonald and Harbaugh, 1988) to add subsidence simulation capabilities to the original Belitz model that did not have this feature. Larson et al. devised three management alternatives that were analyzed over a thirty year period with a probable future drought scenario. The three alternatives included maintaining current practices (as of 2001) and two alternatives that increased groundwater withdrawals. It was found that maintaining

groundwater withdrawals at their existing levels virtually eliminated further land subsidence; however the authors questioned whether this scenario would be sustainable in the long-term due to a growing urban population to the south (with an associated increasing demand on groundwater) as well as ecological reasons for reducing water deliveries from the north.

Faunt (2009) developed the Central Valley Hydrologic Model (CVHM) which is a comprehensive regional-scale modeling surface water and groundwater flow in both the Sacramento and San Joaquin Valleys. CVHM was developed utilizing a comprehensive Geographic Information System (GIS) to analyze data, a texture model to characterize the aquifer stratigraphy, estimates of water budget components of the hydrologic system provided by the FMP, and various simulation capabilities to assess and quantify hydrologic conditions. Subsidence is simulated in CVHM using the SUB package (Hoffmann et al., 2003).

Initial HGSSJVM Development (1961-2003)

Model Parameterization & Calibration – Steady State Conditions

Model parameterization of HGSSJVM was accomplished via transfer of input parameters from CVHM input files to HGS input files. Two types of transfer were implemented depending on the data type of the parameter in HGS. For HGS elemental data, a computer script (referred to herein as the auxiliary parameter transfer program) was developed to search for the CVHM square mile cell containing the HGS element centroid. Then, the parameter value of the CVHM cell was assigned directly to the HGS element in question. For HGS nodal data, another script was developed to locate the four nearest CVHM cells to the HGS node in question. Then, bilinear interpolation was used to interpolate the values from the four CVHM cells onto the HGS node.

Some parameters were also taken directly from Faunt (2009). These procedures were used to populate the HGSSJVM grid with the aquifer properties necessary for the steady-state model (Table 1). The transfer of additional parameters necessary for the transient model will be described in the later section of this report describing calibration under transient conditions. Note that land subsidence is a transient process and therefore cannot be simulated by a steady-state model. Thus, the parameters governing land subsidence (elastic and inelastic skeletal storage, preconsolidation head, and fraction of compressible interbeds) were not transferred from CVHM to HGSSJVM until development of the transient model.

Table 1. Aquifer properties transferred from CVHM to HGSSJVM for steady-state model.

Parameter	Source
Horizontal and Vertical hydraulic conductivity (K_{xx} and K_{zz})	CVHM input arrays of percentage of coarse-grained material (P_c) coupled with statistical relationships correlating P_c with K_{xx} and K_{zz} (USGS PP 1766).
Total Porosity (θ)	CVHM input arrays of percentage of coarse-grained material (P_c) coupled with statistical relationships correlating P_c with θ (USGS PP 1766).

The initial head in the aquifer was set equal to the land surface elevation. The lateral boundaries were assumed to have a no flow boundary condition, with the exception of a portion of the northwest corner of the model domain which was assumed to have a constant head of zero (i.e., sea level). This boundary correlates with a portion of the boundary of the Sacramento-San Joaquin Delta and the San Joaquin basin. This boundary condition (BC) provides the boundary with an outlet of water (Figure 1). The BC specifications are consistent with CVHM.

Since this version of HGSSJVM is treating the subsurface portion of the model domain solely, surface-subsurface fluid exchange was treated via explicit specifications of infiltration and exfiltration over the ground surface. It is noted that recharge takes place at the water table, and discharge into the Delta takes place along the flow boundary north of the San Joaquin basin. Unsaturated flow is still represented via solution of Richards' equation and implementation of the HGS "pseudo-soil" function, which is an adaptation for unstructured finite element grids of the method by Huyakorn et al. (1994). In this approach in HGS, relative permeability of aquifer materials at the nodes is set equal to nodal saturation, and saturation values of the soils and aquifer materials are correlated with pressure head. Saturation values are restricted to the range 10^{-3} to unity. In other words, the maximum saturation is the physical limit of full saturation but the minimum saturation is 10^{-3} instead of zero. Strictly speaking, this introduces a small bias that theoretically could alter model estimates of processes such as recharge (compared to FMP, for example) but it is assumed that the minimum saturation of 10^{-3} is small enough such that any resulting bias is expected to be negligible.

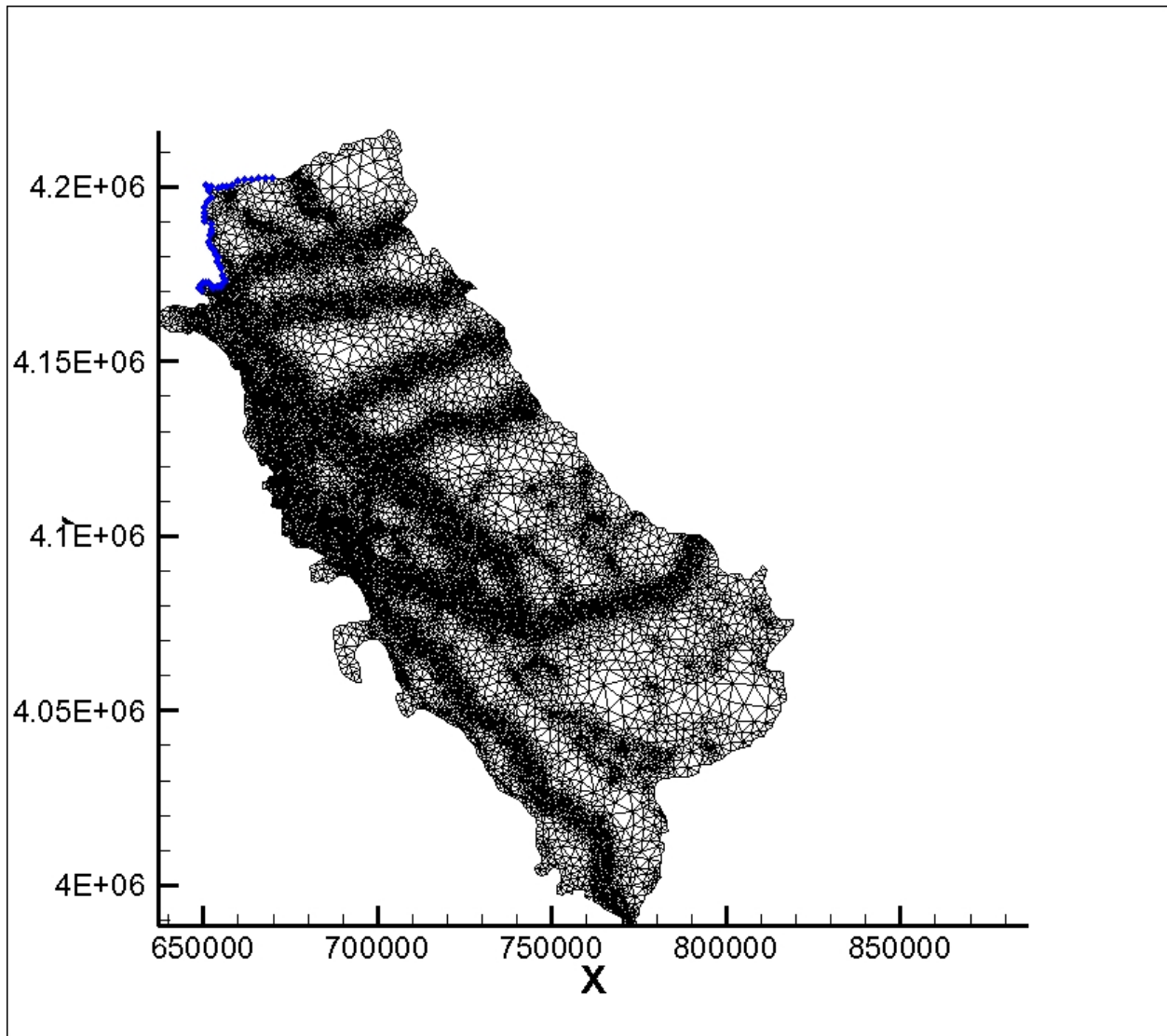


Figure 1. HGSSJVM model grid. Blue nodes = boundary with a constant head BC

Recharge from the surface into the subsurface is also represented as focused recharge along the river reaches descending from the mountains and through the foothills towards the valley floor, as well as from excess irrigation water (i.e., the fraction not consumed by evapotranspiration). Note that this implies the assumption that recharge occurs via infiltration. Six infiltration zones were created corresponding to the six major rivers (Stanislaus, Tuolumne, Merced, Chowchilla, Fresno, and San Joaquin) descending from the eastern side of the model domain, as well as an additional zone in the southwestern corner of the model domain that corresponds to the Lost Hills region. The infiltration zones for each river extend western from the eastern model boundary to the edge of the valley floor (thus representing the natural recharge associated with the rivers). In the north-south direction, they are continuous. Infiltration was specified for the six river zones according to their relative long term flow rates. These relative weights remained constant while the infiltration flux for the San Joaquin River (the one with the largest long-term average flow rate) was used as a calibration parameter. The additional infiltration zone in the southwestern corner was also used as a calibration parameter. It is important to note that this initial step of the model development was intended to create a basic model construction such that the fundamental hydrogeology and

aquifer parameters of the SJV were captured. Thus, the creation of these infiltration zones represents the natural (predevelopment) conditions of recharge being associated with the major rivers feeding the valley, plus the Lost Hills region. Note that there is no recharge due to infiltration of irrigation water in the steady-state model, because the steady-state conditions correspond to the predevelopment state of the system prior to the introduction of major agricultural development.

Discharge from the subsurface onto the surface was assumed to occur along the river reaches traversing the valley floor. Eight discharge zones were defined, and each one was treated as a calibration parameter although five of the eight zones finished with the same calibrated value of discharge flux for their final calibrated values. Zones 1 through 8 cover the majority of the valley floor going from north to south, respectively. In the final calibration, the mean flux of water into the subsurface (averaged over the entire model domain including areas with no explicit specifications of infiltration) was 1.00 mm/day. The mean flux out of the subsurface (averaged over the entire model domain) was 0.55 mm/day. The difference in these fluxes (0.45 mm/day) represents the outflow across the boundary defined by the constant head BC in the northwest corner into the Delta, plus any evaporation and evapotranspiration (ET) occurring throughout the model domain. The final calibrated infiltration and exfiltration values for each zone are given in Table 2.

Vcdn

Zone	Specified Flux [mm/day]
Discharge zones 1	-1.25
Discharge zone 2	-1.50
Discharge zone 3	-1.75
Discharge zone 4-8	-2.00
Stanislaus River	3.83
Tuolumne River	5.25
Merced River	3.18
Chowchilla River	0.30
Fresno River	0.32
San Joaquin River	6.00
Southwestern corner	4.20

The HGSSJVM simulation results compare favorably with the estimated predevelopment water table elevations given in USGS Professional Paper 1401-D. Figure 3 presents a map comparing the simulated water table elevations with the estimated (i.e., “observed”) water table elevations. One can see that the “observed” and simulated contours match reasonably well and both indicate the same patterns of flow, which, in general, go from east to west following the main rivers flowing down from the Sierra Nevada mountains, and then south to north along the trough of the valley following the trajectory of the San Joaquin River towards the Sacramento-San Joaquin Delta. One can also notice a correlation between land surface elevation and water table elevation. Figure 4 presents a scatter plot of “observed” (or estimated) and simulated water table elevations. To

construct this plot, one hundred (x,y) locations were selected from the entire extent of the model domain in an approximately uniform manner. In other words, the one hundred locations were selected by eye to ensure the entire model domain was well represented. Their spatial distribution is not exactly uniform (and it would be impossible to achieve exact uniformity) because of the variable grid resolution. Relevant statistics from the scatter plot include a mean residual error of -2.3 m and a mean absolute residual error of 4.7 m. The latter statistic corresponds to 4.8% of the spread in observed values, indicative of a successful calibration (i.e., < 5%).

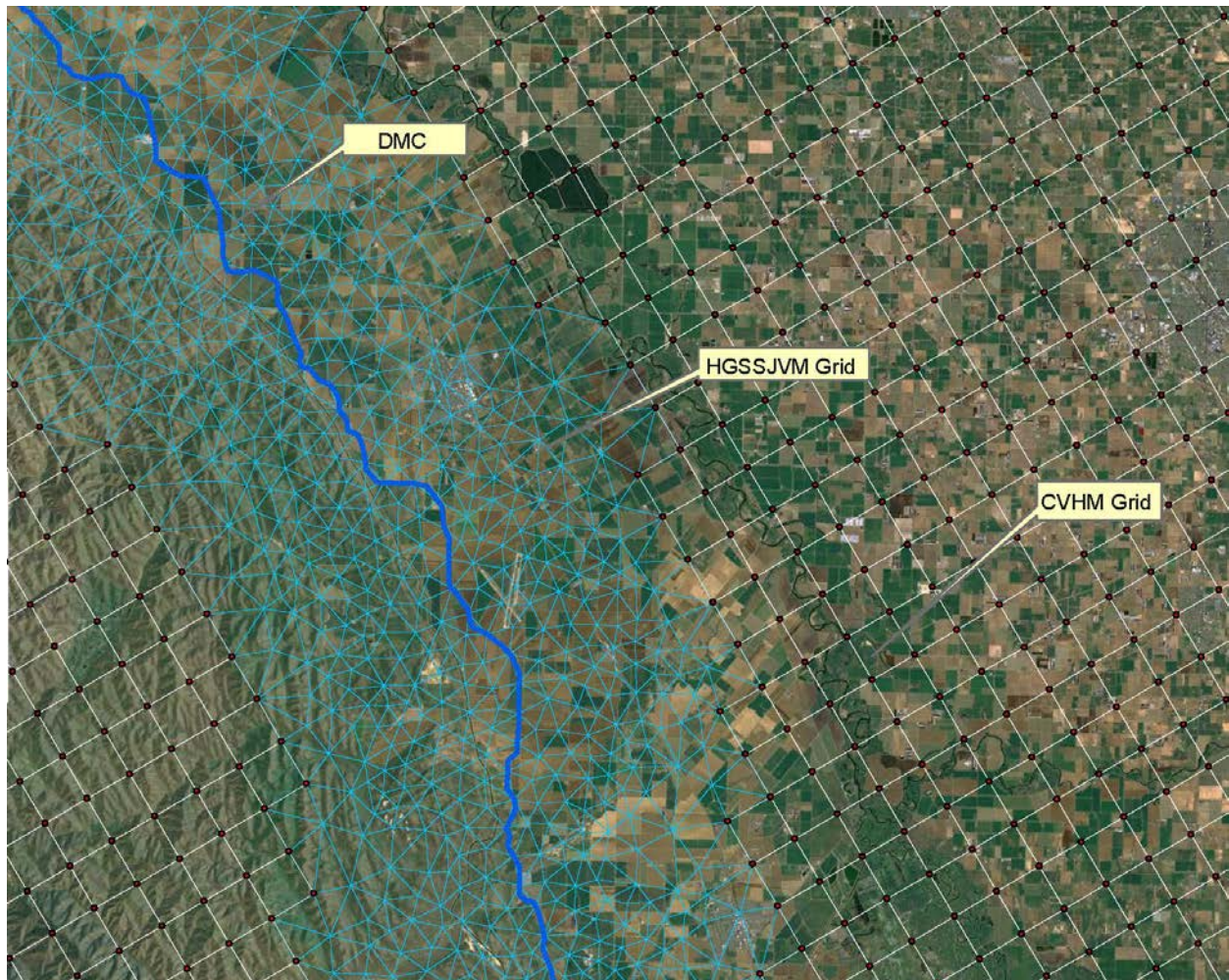


Figure 2. Refinement of HGSSJVM Grid near the Delta-Mendota Canal.

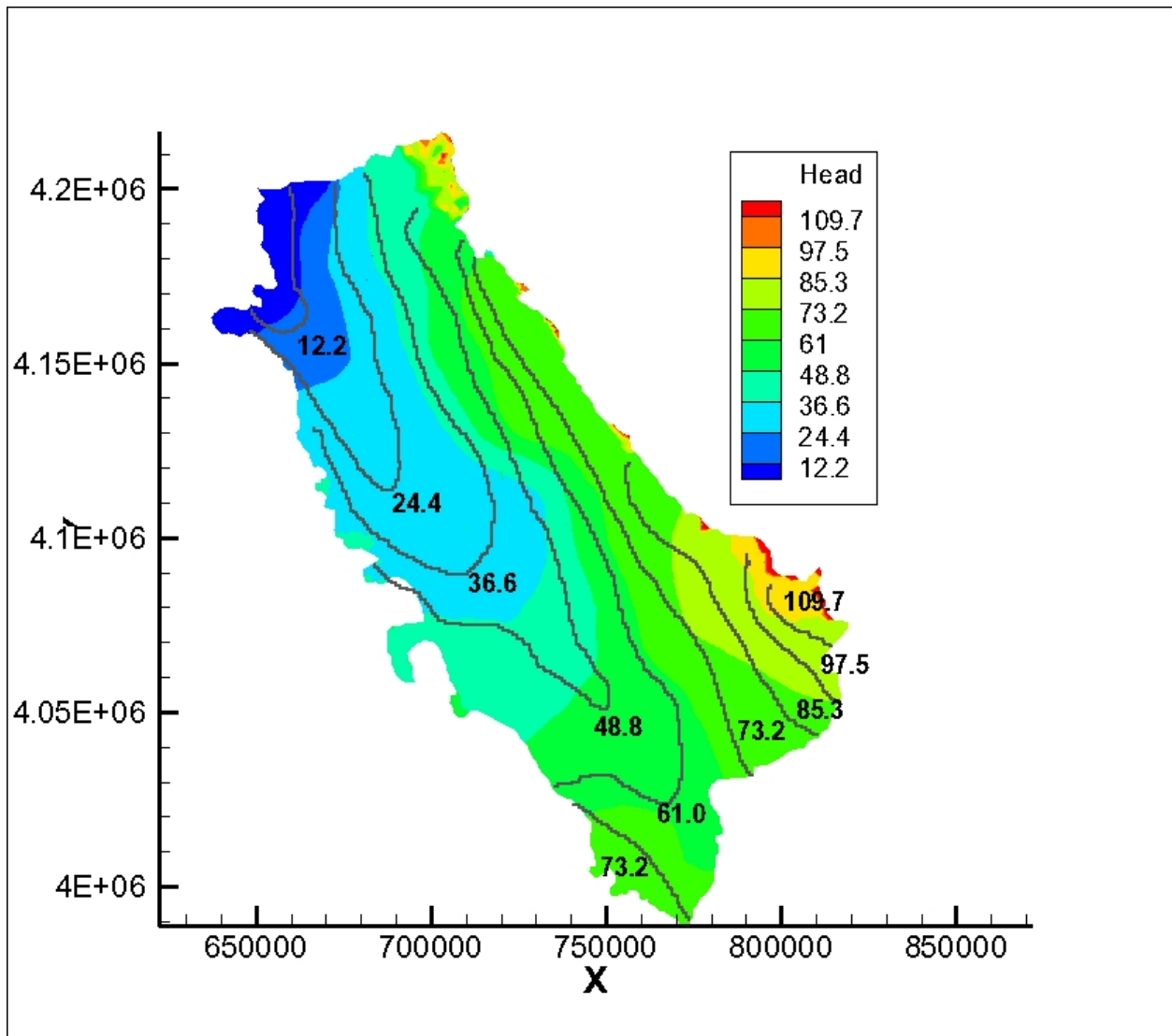


Figure 3. Contour plot comparing observed water table elevations versus HGSSJVM simulated water table elevations.

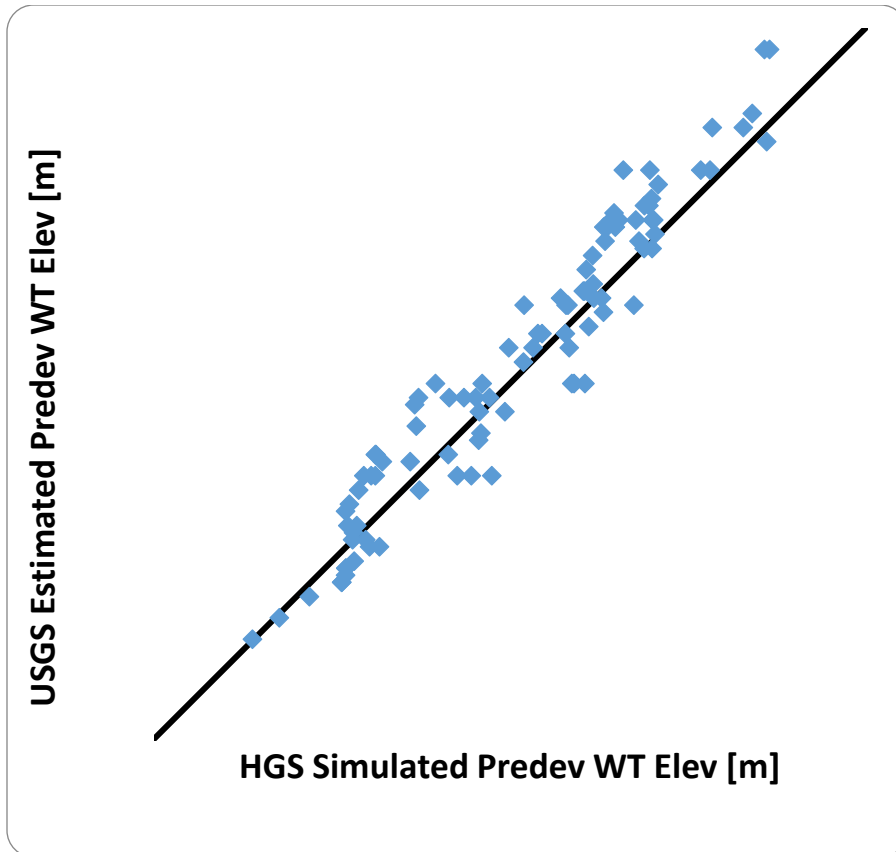


Figure 4. Scatter plot comparing observed water table elevations versus HGSSJVM simulated water table elevations.

The steady-state calibration of HGSSJVM, via manual adjustment of infiltration/exfiltration between the aquifer and land surface, suggests that the model that has been developed from this basic steady-state model parameterization represents the fundamental hydrogeological processes of the San Joaquin Valley. While the data is not available for a more precise and detailed calibration for the case of natural predevelopment conditions, this exercise indicates that HGSSJVM appears to capture the dominant processes of subsurface flow. Also, the ability to achieve good agreement with the USGS estimated predevelopment water table without any adjustment of hydraulic conductivity values suggests that these conductivity values obtained from the CVHM model provide a reasonable representation of the subsurface hydraulic properties (as expected since the source of these parameters is the calibrated CVHM). The next step was to perform a transient calibration using available groundwater head and compaction measurements from the period 1961-2003, during which the aquifer system was under dramatic and dynamic anthropogenic stresses (as well as several significant periods of drought) owing to the agricultural development of the San Joaquin Valley, the initial reliance on groundwater pumping for irrigation, and then the eventual importation of surface water deliveries from reservoirs to the east and north. Achieving a successful transient calibration will increase the utility of HGSSJVM for detailed studies of the effects of groundwater pumping on potential land subsidence in the San Joaquin Valley.

HGSSJVM Model Calibration – Transient Conditions

Initial model parameterization for the transient model was accomplished in similar fashion to the steady-state model via transfer of input parameters from CVHM input files to HGS input files based on the two different spatial matching algorithms for elemental and nodal data. The additional data required for the transient model can be separated into physical parameters and anthropogenic parameters (all parameters will be defined below). The physical parameters include specific storage, elastic skeletal specific storage, inelastic skeletal specific storage, fraction of compressible interbeds, initial heads, preconsolidation heads, precipitation and evapotranspiration (ET). The anthropogenic parameters include groundwater pumping, applied irrigation water from groundwater pumping, and applied irrigation water from surface water deliveries. Precipitation and ET as well as all of the anthropogenic parameters required consideration of both the temporal as well as spatial distribution of values. The simulation period for the transient model is April, 1961 through September, 2003 (same period as CVHM) with monthly time steps for the transient parameters. Note that the computational time step for HGS is adaptive and not necessarily the same as the constant monthly step used for the stresses. However, these monthly stresses constrain the HGS computational time step such that it is always less than or equal to one month.

Specific storage is the amount of water released or taken into storage per unit volume of a porous medium per unit change in head. Elastic skeletal specific storage is the amount of water released or taken into storage per unit volume of a porous medium per unit change in aquifer compression due to elastic (i.e., reversible) deformation of the aquifer matrix. Inelastic skeletal specific storage is the amount of water released or taken into storage per unit volume of a porous medium per unit change in aquifer compression due to inelastic (i.e., irreversible) deformation of the aquifer matrix. Fraction of compressible interbeds is the fraction of aquifer material composed of compressible fine-grained materials. Initial heads refer to the initial piezometric heads (equal to the water table under unconfined conditions) in the aquifer at the simulation start time. Preconsolidation heads refer to the minimum groundwater head values experienced at any given point in the aquifer prior to the given point in time; these values were taken from CVHM directly for initializing the model. If in the course of a model simulation a lower head value is obtained, then the preconsolidation head value is updated accordingly. Precipitation is the amount of rainfall intercepted by the land surface. Evapotranspiration is the amount of water removed from the land surface and transported to the atmosphere, equivalent to the sum of evaporation and plant transpiration. Groundwater pumping is the volume of water per month pumped from either the semi-confined or confined aquifers by groundwater wells for any purpose. Applied irrigation water from groundwater pumping and surface water deliveries is the volume of water per month applied to the land surface for agricultural purposes from each source.

The representation of groundwater pumping in the transient HGSSJVM was accomplished by transferring the spatially and temporally distributed pumping values from CVHM. The authors of CVHM developed estimates for agricultural and urban pumping as follows (Faunt, 2009). For every CVHM model cell of one square mile where an irrigated crop was the predominant land use for the given month, a single well was placed in the model cell. This placement strategy included spatial variation both horizontally and vertically by placing wells in the different CVHM model layers based on available well log data for the relevant areas. Urban wells were placed in model cells (and for given months) where (and when) urban water use (municipal or industrial) was the predominant use of pumped groundwater. The pumping rates for agricultural wells were estimated

as the difference between irrigation water requirements and surface water deliveries. Irrigation water requirements were estimated by the auxiliary Farm Package program (Schmid et al., 2006), and surface water deliveries were based on historical data. Urban pumping rates in CVHM were based on unpublished historical records provided to the USGS by the California Department of Water Resources (DWR).

The transfer of the spatiotemporal groundwater pumping values in CVHM into HGSSJVM was not straightforward. Aggregation of many of the CVHM representative wells (which in general represent an aggregation of actual, individual wells) was necessary for the following reasons: the HGS code is unable to represent more than approximately 1200 wells due to memory allocation constraints; HGS is unable to define different wells at the same location at different points in time; the variable grid size of the HGSSJVM grid is not able to resolve every square mile well placement from CVHM. Thus, an auxiliary program was written to merge CVHM agricultural and urban wells that exist in the same location but at different times and multiple CVHM wells that are associated with the same HGSSJVM node in the coarser areas of the HGSSJVM grid. Additionally, CVHM wells that existed in more than one sub-Corcoran layer were merged, and the same was done for wells existing in more than one layer above the Corcoran clay; thus, HGSSJVM contains only one well placed above the clay and one well placed below the clay for each (x,y) location. This final type of merge was implemented to bring the number of wells down to a quantity that could be handled by HGS. The final number of wells resulting from this merging and transfer methodology was 1023. The resulting distribution of wells in the (x,y) plane is depicted in Figure 5.

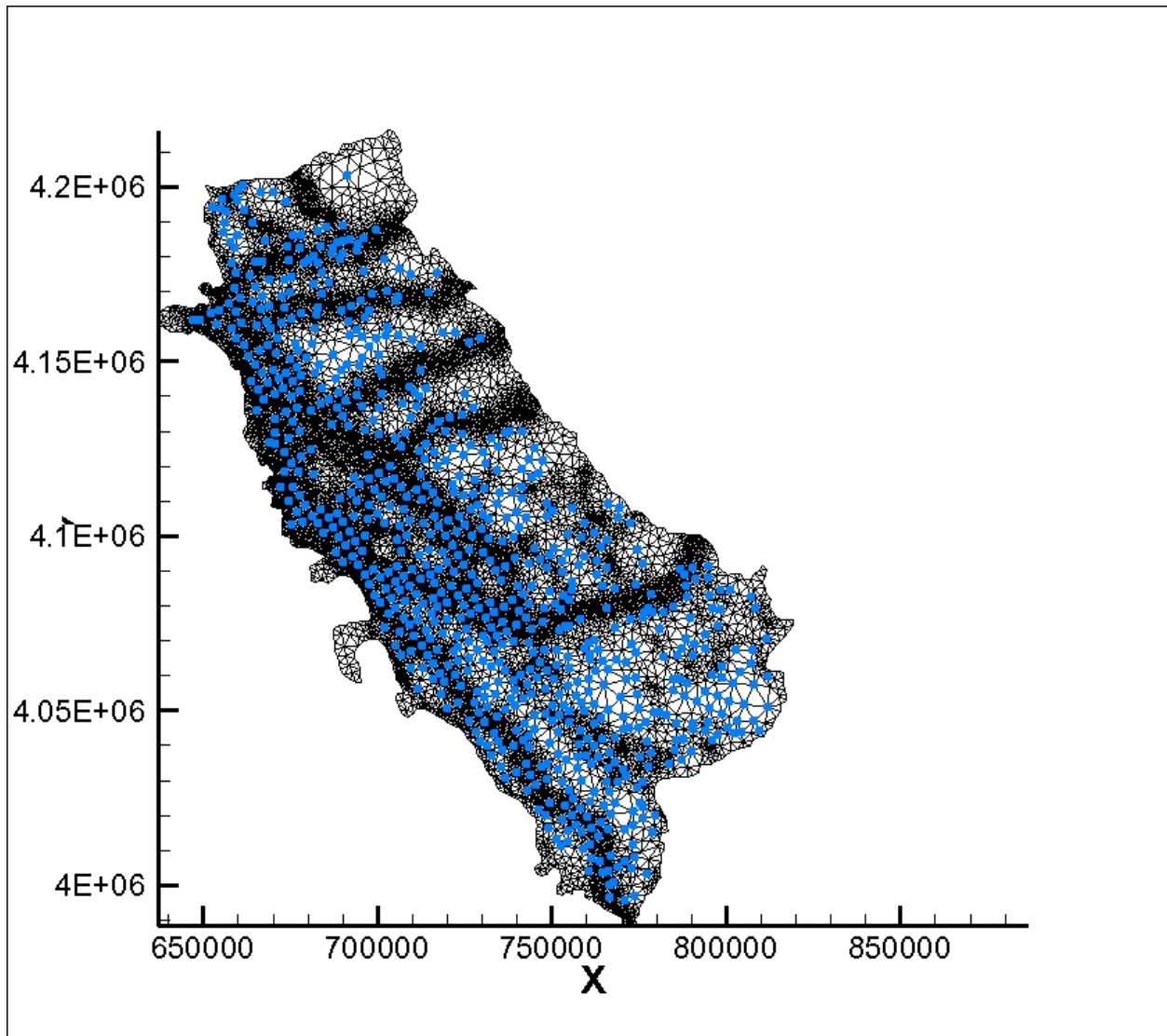


Figure 5. Distribution of groundwater well locations in HGSSJVM

The initial heads in the aquifer for the transient HGSSJVM were transferred directly from CVHM using an auxiliary program written for this purpose. This auxiliary program cycles through every element in HGSSJVM and matches the element centroid with the closest CVHM model cell. Then, the initial head from the CVHM cell is transferred to the corresponding HGSSJVM element. As previously described (Faunt, 2009), sufficient historical water levels were not available until the 1960's which makes the choice of initial conditions problematic since the combined effects of irrigation and groundwater pumping greatly increased vertical head gradients in the San Joaquin Valley; this is because recharge from irrigation increases the heads near the top of the aquifer while pumping tends to decrease heads at lower depths in the aquifer. Due to the gradients thus created, the system was still in a transient state in the middle of responses to stresses prior to 1960. To resolve this difficulty, the initial heads in CVHM were determined by using historical heads for April, 1961 and then allowing the model to run forward for a year thus dissipating the transient effects of the poorly estimated initial heads. These heads that were obtained after a one year simulation period were then defined as the set of initial heads corresponding to the April, 1961

simulation start time. These initial heads determined for the CVHM model were transferred to HGSSJVM by the algorithm previously described.

Just as in the steady-state HGSSJVM, most of the lateral boundaries were assumed to have a no flow boundary condition, with the exception of a portion of the northwest corner of the model domain which was assumed to have a constant head of zero (i.e., mean sea level). This boundary correlates with a portion of the boundary of the Sacramento-San Joaquin Delta and the San Joaquin basin. This boundary condition provides the one location for outflow from the model domain (Figure 1).

Similarly to the steady-state HGSSJVM, surface water-groundwater interaction was treated via explicit specifications of infiltration and exfiltration along the ground surface. For the transient model, the CVHM spatiotemporal values for precipitation, ET, and surface water deliveries (for irrigation) were transferred to HGSSJVM via the auxiliary parameter transfer program (described in the section above). Spatially, each value represents the sum of the flux in question over one of the ten water balance subregions (regions 8-17) that are coincident to both CVHM and HGSSJVM (see, e.g., Figure A8 in Faunt, 2009). Then, a net recharge value was obtained by summing the precipitation and surface irrigation and subtracting the ET for each subregion and each month in the simulation period. For irrigation from groundwater wells, a separate algorithm was developed so that the irrigation being simulated would be consistent with the agricultural wells as represented in HGSSJVM following the transfer and aggregation of CVHM wells. In other words, the process of aggregating and transferring CVHM wells into HGSSJVM means that there is not a one-to-one correspondence between CVHM and HGSSJVM agricultural wells. Thus, for internal model consistency, rather than taking groundwater well irrigation directly from CVHM, these irrigation values were determined from the agricultural wells that were ultimately placed in HGSSJVM following the aggregation and transfer process. This method of assigning irrigation water from groundwater sources in an internally consistent manner with the way that HGSSJVM agricultural groundwater wells were defined is based on the assumption that groundwater used for irrigation is applied in close proximity to the wells from which it is extracted. Thus, the internally consistent method ensures that the extracted agricultural groundwater being simulated in HGSSJVM is applied in the vicinity of the wells from which it is being pumped.

To calibrate the transient HGSSJVM for the purpose of representing the subsurface hydrology and response of the compressible aquifer matrix to the stresses imposed by groundwater pumping, a subset of the data used to calibrate CVHM was selected. The calibration data selected consisted of two types: historical groundwater levels and historical compaction (both elastic and the inelastic compaction that results in subsidence). Calibration target locations were selected with a focus on the area surrounding the Delta-Mendota Canal (due to the intended initial application of analyzing land subsidence in the DMC area) but also distributed throughout the model domain. Substantial manual calibration was pursued to ascertain reasonable first guesses for the calibration parameters prior to using the PEST software (Doherty, 2002) for automated calibration. The calibration parameters included the magnitude of the coarse and fine hydraulic conductivity values (K_{ch} , K_{fh} and K_{cv} , K_{fv} respectively) and the exponent parameters (p_h and p_v , respectively) of the horizontal and vertical hydraulic conductivity statistical distributions. The spatial variation in hydraulic conductivity was dictated by the fraction of coarse-grained material which was transferred to HGSSJVM via the auxiliary parameter transfer program. Then, when the conductivity and

exponent parameter values were varied, the auxiliary program was utilized to generate the new hydraulic conductivity field. The specific storage values were treated in a similar manner with coarse (Ss_c) and fine (Ss_f) values but the exponent parameter was held constant at unity. For the other calibration parameters, the manual calibration included different configurations of the spatial distribution. The configurations resulting from the manual analysis were as follows: four values of the inelastic skeletal storage coefficient, and one value of the elastic skeletal storage coefficient. For the inelastic skeletal storage coefficients, separate values were calibrated for the sub-Corcoran layers, the two Corcoran clay layers, and aquifer material above the clay; the uppermost five shallow layers were combined for assignment of one coefficient. For the elastic skeletal storage coefficients, one value was assigned everywhere. In Tables 4 and 5, the numerical subscripts on the specific storage parameters are in ascending order corresponding to the associated model layers (individual or aggregated) going from top to bottom. Ssi refers to inelastic skeletal specific storage, Sse refers to elastic skeletal specific storage, and Ss refers to specific storage.

Table 3. Calibration parameter values following manual calibration.

<u>Parameter</u>	<u>Initial Guess for PEST</u>
Kch	396 m/day
Kfh	0.01 m/day
ph	0.39
Kcv	280 m/day
Kfv	23 m/day
pv	0.25
Ssc	$5.0 * 10^{-3} m^{-1}$
Ssf	$1.7 * 10^{-1} m^{-1}$
Ssi1	$1.0 * 10^{-4} m^{-1}$
Ssi2	$1.2 * 10^{-4} m^{-1}$
Ssi3	$5.0 * 10^{-4} m^{-1}$
Ssi4	$1.1 * 10^{-6} m^{-1}$
Sse	$2.0 * 10^{-7} m^{-1}$

Table 4. Calibration parameter values following PEST calibration.

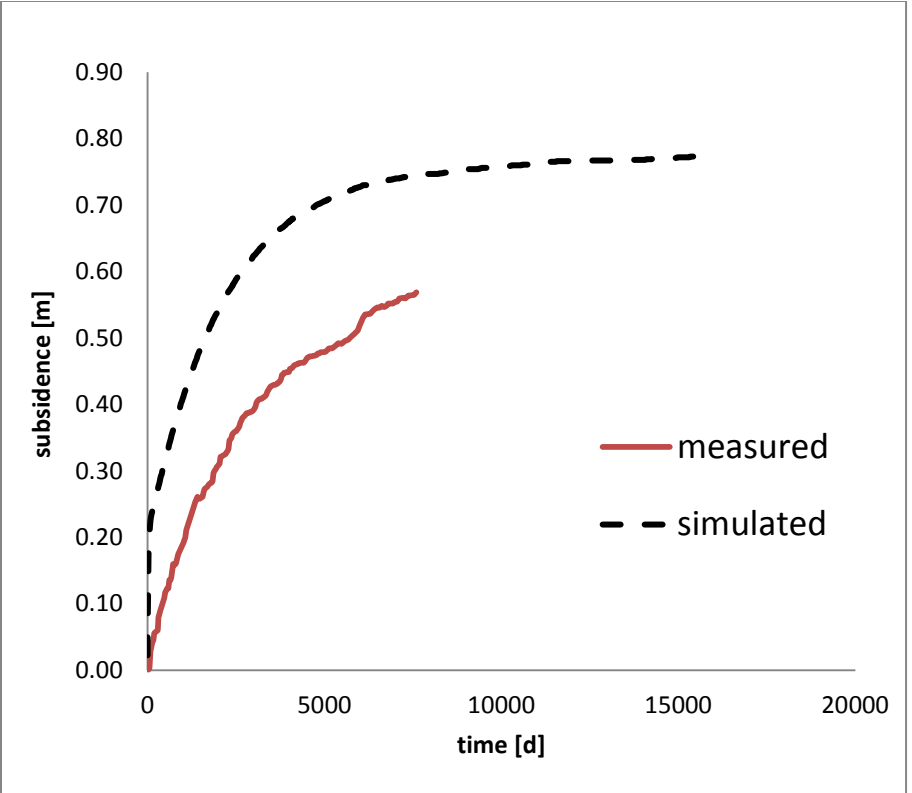
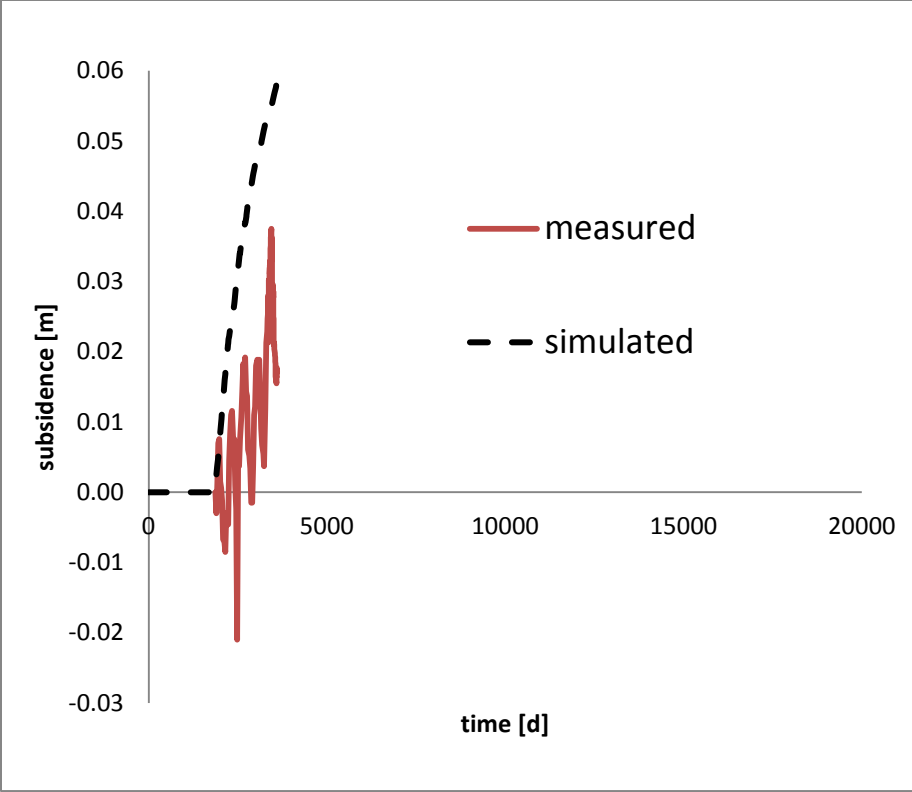
<u>Parameter</u>	<u>Initial Guess for PEST</u>
Kch	348 m/day
Kfh	14.93 m/day
ph	0.0011
Kcv	200 m/day
Kfv	14.26 m/day
pv	0.9867
Ssc	$1.0 * 10^{-3} m^{-1}$
Ssf	$1.8 * 10^{-1} m^{-1}$
Ssi1	$1.0 * 10^{-4} m^{-1}$
Ssi2	$1.2 * 10^{-4} m^{-1}$
Ssi3	$5.0 * 10^{-4} m^{-1}$
Ssi4	$1.1 * 10^{-6} m^{-1}$
Sse	$2.0 * 10^{-7} m^{-1}$

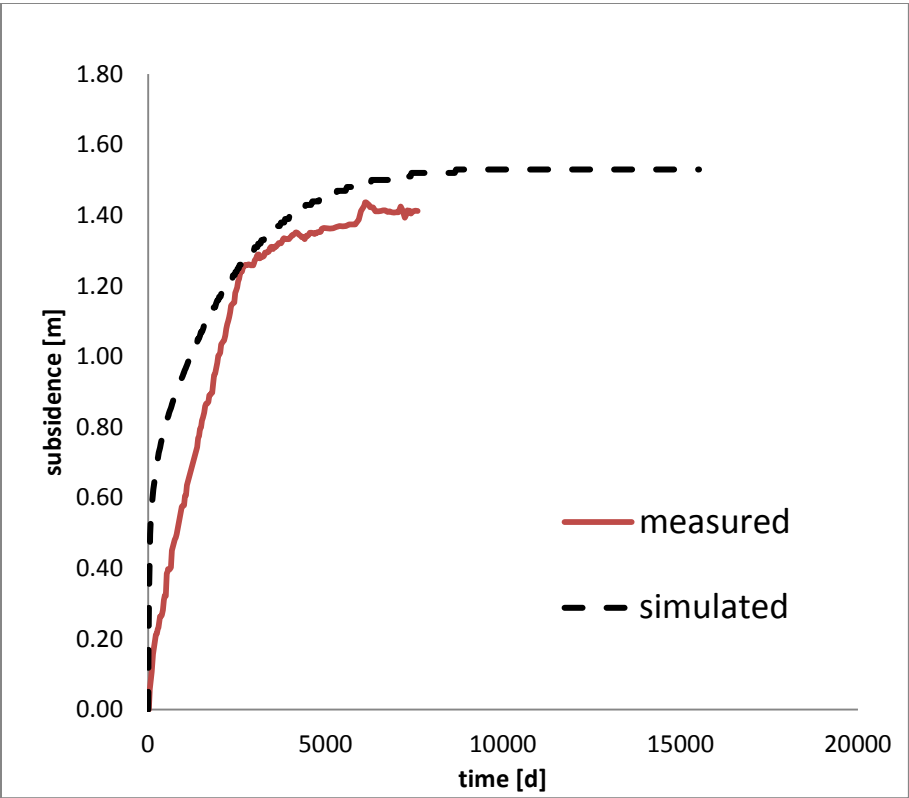
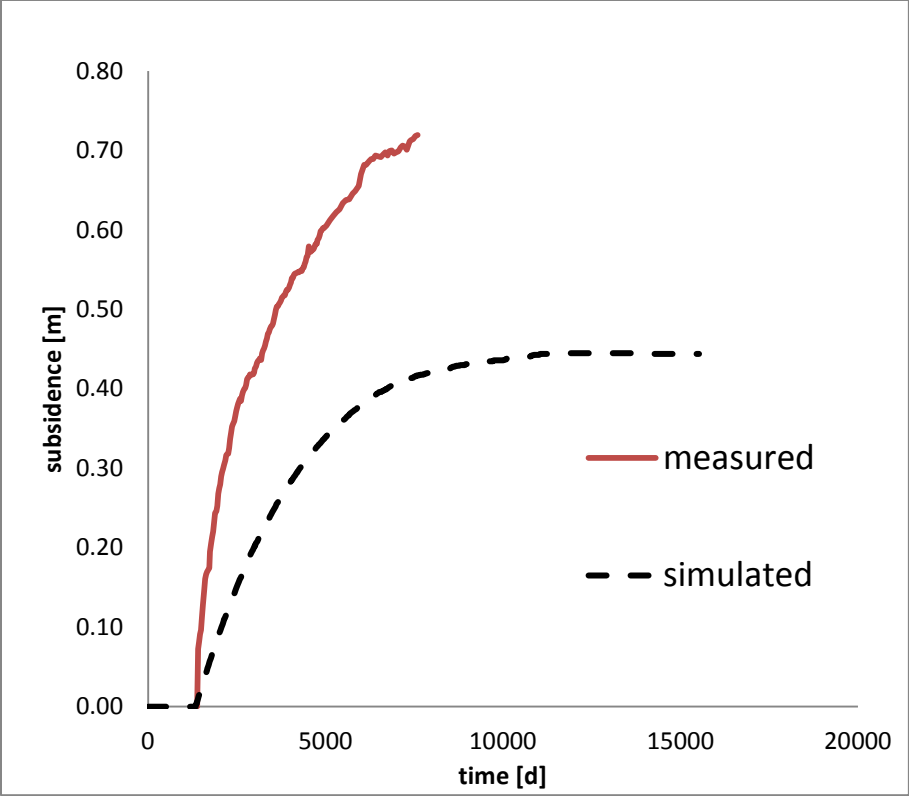
Following the manual calibration, an automated calibration procedure was performed with PEST. PEST takes an initial set of guesses for all of the model's calibration parameters (e.g., those parameters listed in Tables 4 and 5), runs the model and then measures the residual between the simulated values of the calibration targets (e.g., heads and compaction) and the observed values. PEST then uses the method of Gauss-Marquardt-Levenberg to adjust the calibration terms with the objective of minimizing the sum of the squares of all the residuals; this particular method used by PEST is applicable to nonlinear problems. PEST repeats the process of adjusting the calibration parameters and re-running the simulation until the residuals are minimized to within a specified tolerance or no further improvement is being achieved. The adjusted calibration parameters obtained from using PEST in this fashion are listed in Table 5. Note that all of the inelastic and elastic skeletal storage parameters were relatively insensitive to further variations in PEST and thus remained the same as the manually calibrated values.

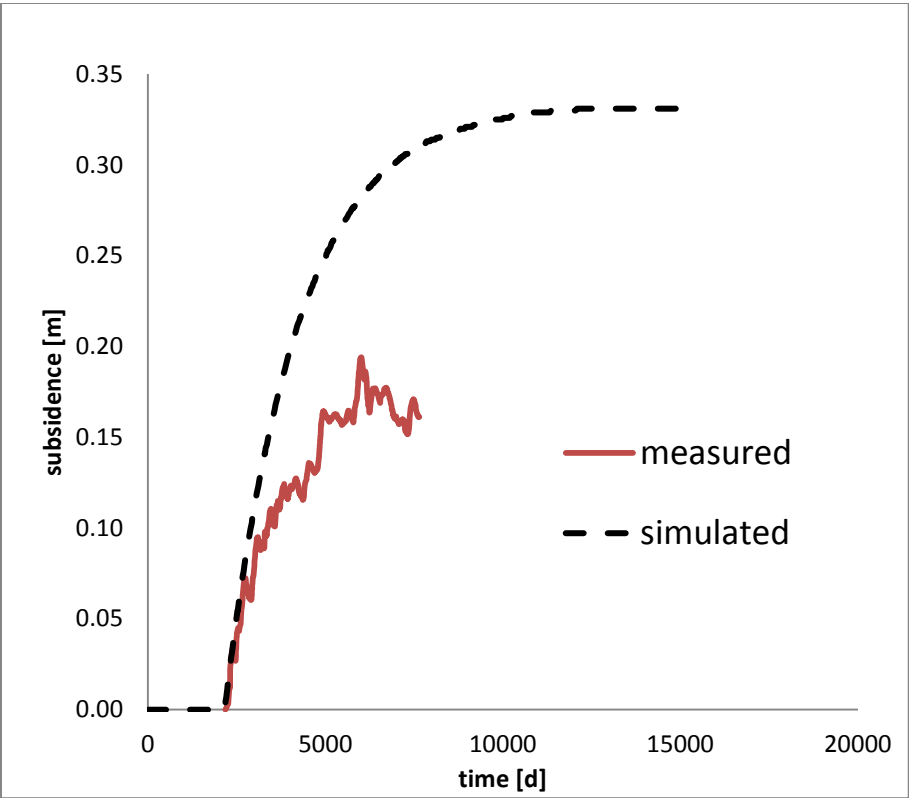
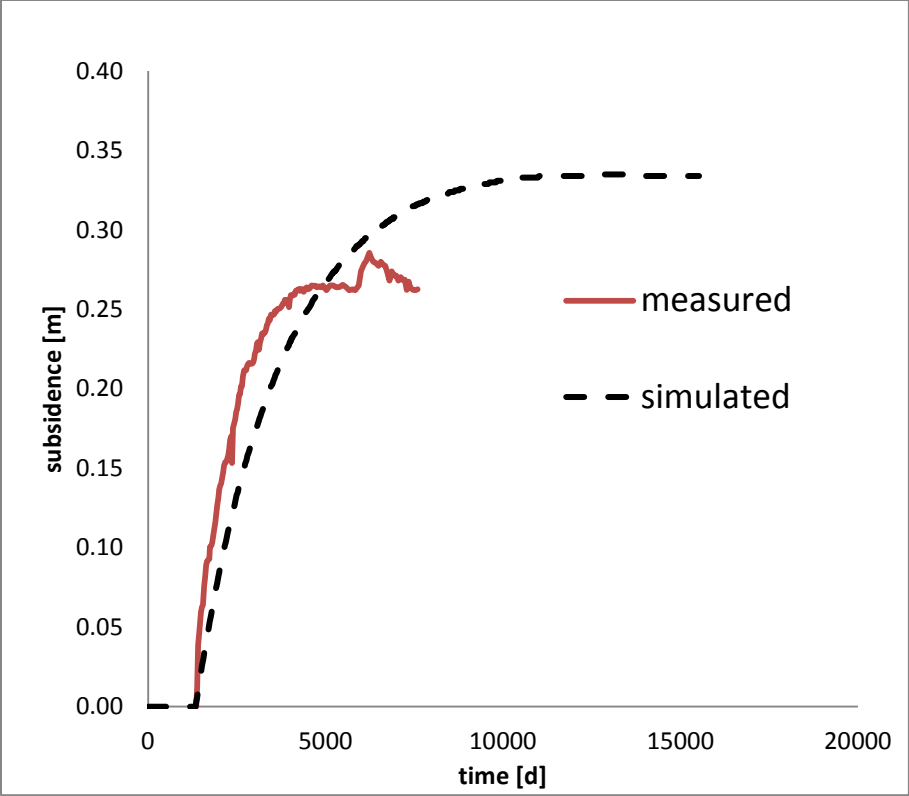
The manual calibration began with initial guesses based on CVHM values of the relevant parameters. Following the manual calibration, the initial guesses for these parameters (Table 4) were supplied to the automated calibration program PEST which automatically varies the parameters and searches for the optimal parameter set to minimize the objective function which is defined as the sum of the squared residuals (i.e., differences between measured observations and model simulations). The final calibrated parameters for the model are listed in Table 5.

The calibration period (7639 days) was selected to be approximately half of the total simulation period (15520 days) in order to retain the latter half of the observation data for model verification and validation. The manual calibration resulted in an improved fit compared to the initial guesses based on CVHM values and the PEST calibration yielded further improvement, thus achieving the objective of a calibrated model based the commonly accepted criterion of the root mean square deviation (RMSD) being < 10% of the range in observed values. This criterion was met for both water levels and subsidence values for both the calibration period and the verification period. For the calibration period, the water level RMSD was 4.9% of the range of the observed values and the subsidence RMSD was 9.8% of the range of the observed values. When the model was run for the entire verification period, the water level RMSD was 6.3% of the range of the observed values and the subsidence RMSD was 9.8% of the range of the observed values.

Figure 6 shows the calibrated (simulated) subsidence values compared to the observed values at the seven monitoring locations in the vicinity of the DMC. Visual inspection of the agreement between simulated and measured values suggests that the model represents the basic relationship between groundwater pumping and land subsidence in the Western San Joaquin Valley.







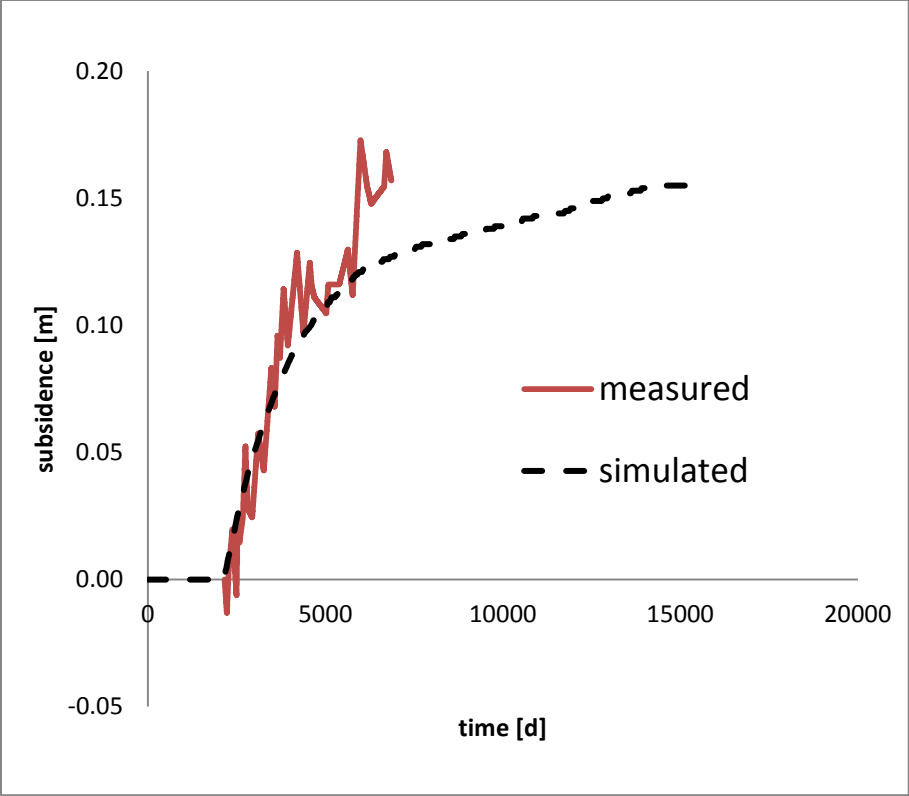


Figure 6. Measured and simulated subsidence at locations near the Delta-Mendota Canal

Preliminary Analysis of Land Subsidence/Groundwater Pumping Relationship In the Vicinity of the DMC

Baseline Model

The baseline model for the preliminary analysis is defined as the final calibrated HGSSJVM defined in the preceding section with the associated groundwater levels and subsidence values for the April, 1961 through September, 2003 simulation period.

Model Scenarios

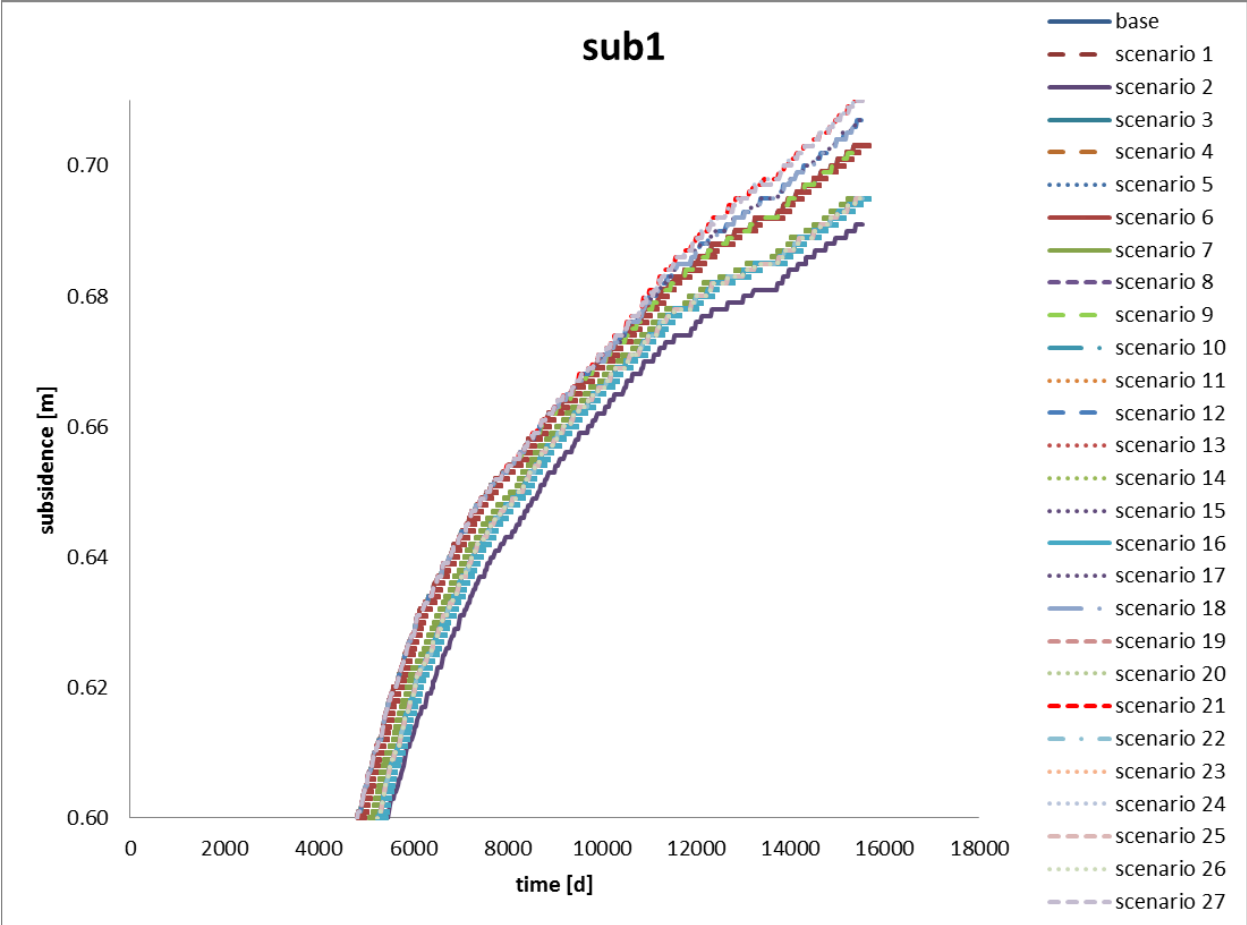
For an initial analysis of the land subsidence/groundwater pumping relationship in the portion of the Western San Joaquin Valley near the DMC, an ensemble of model scenarios was developed with the intention of probing the effects of three different factors on the resulting subsidence: (1) location of pumping along the DMC; (2) timing of pumping within the irrigation season; (3) overall magnitude of pumping. For each factor, three different cases were considered. For location, three subsets of wells expected to pump into the DMC under the Warren Act were assembled corresponding to the Northern, Central, and Southern portions of the DMC. For timing, the three cases were for all pumping to occur in one of three different two-month periods: (1) May/June; (2) July/August; (3) September/October). For magnitude, the chosen magnitudes were 50,000 acre-ft, 75,000 acre-ft, and 100,000 acre-ft. These magnitudes of pumping represent additional pumping that is incorporated into the model above the baseline pumping that was set in the baseline model for the April, 1961 through September, 2003 period. This enables a comparative analysis that looks at whether the additional pumping results in any additional subsidence over and above the historical baseline model subsidence. The additional pumping represented in the model scenarios occurs only in the below normal, dry, and critical years of the historical model simulation period. By combining all possible combinations of the three factors, a total of 27 scenarios were defined. The resulting scenarios are listed in Table 3.

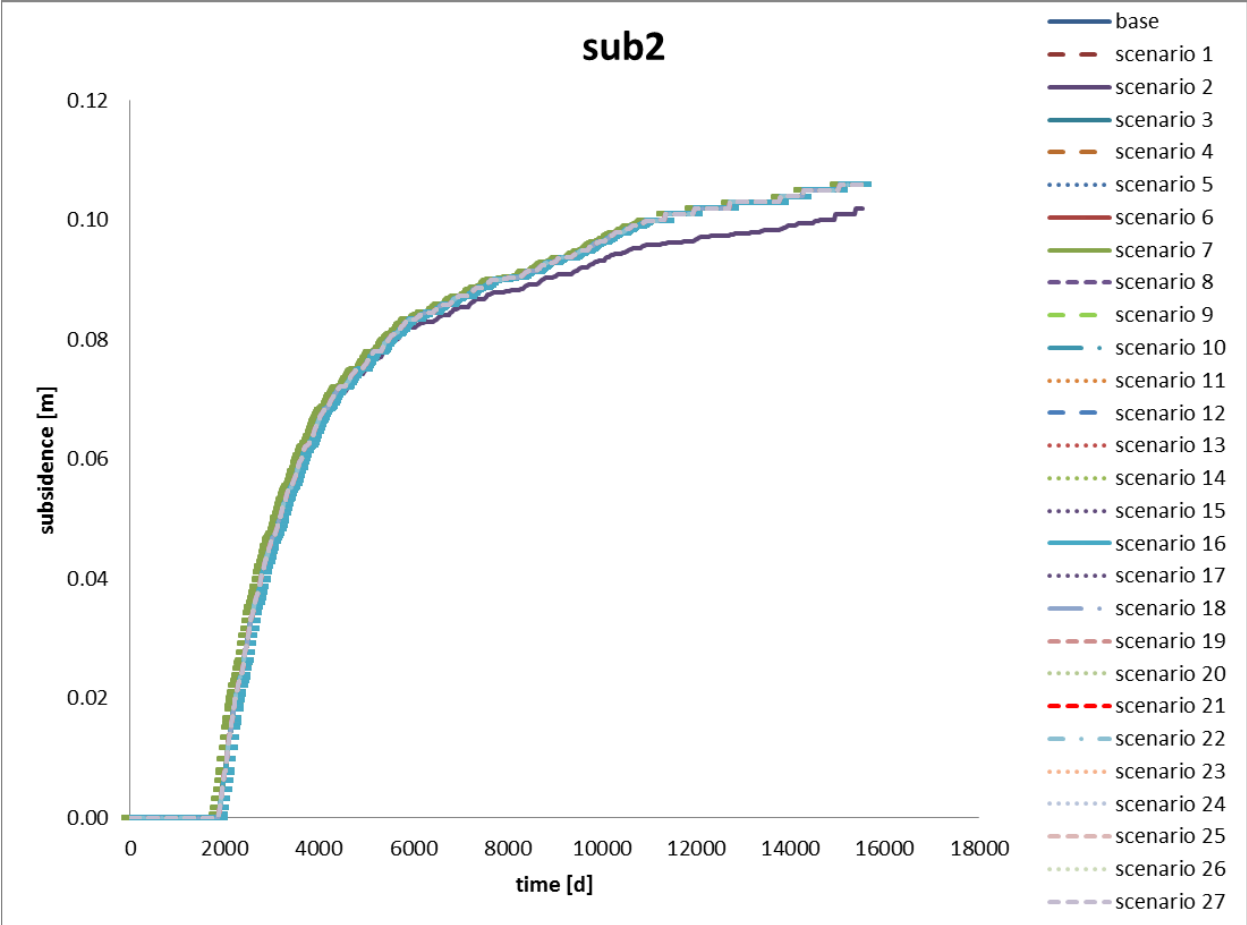
Table 5. Preliminary Analysis Model Scenarios

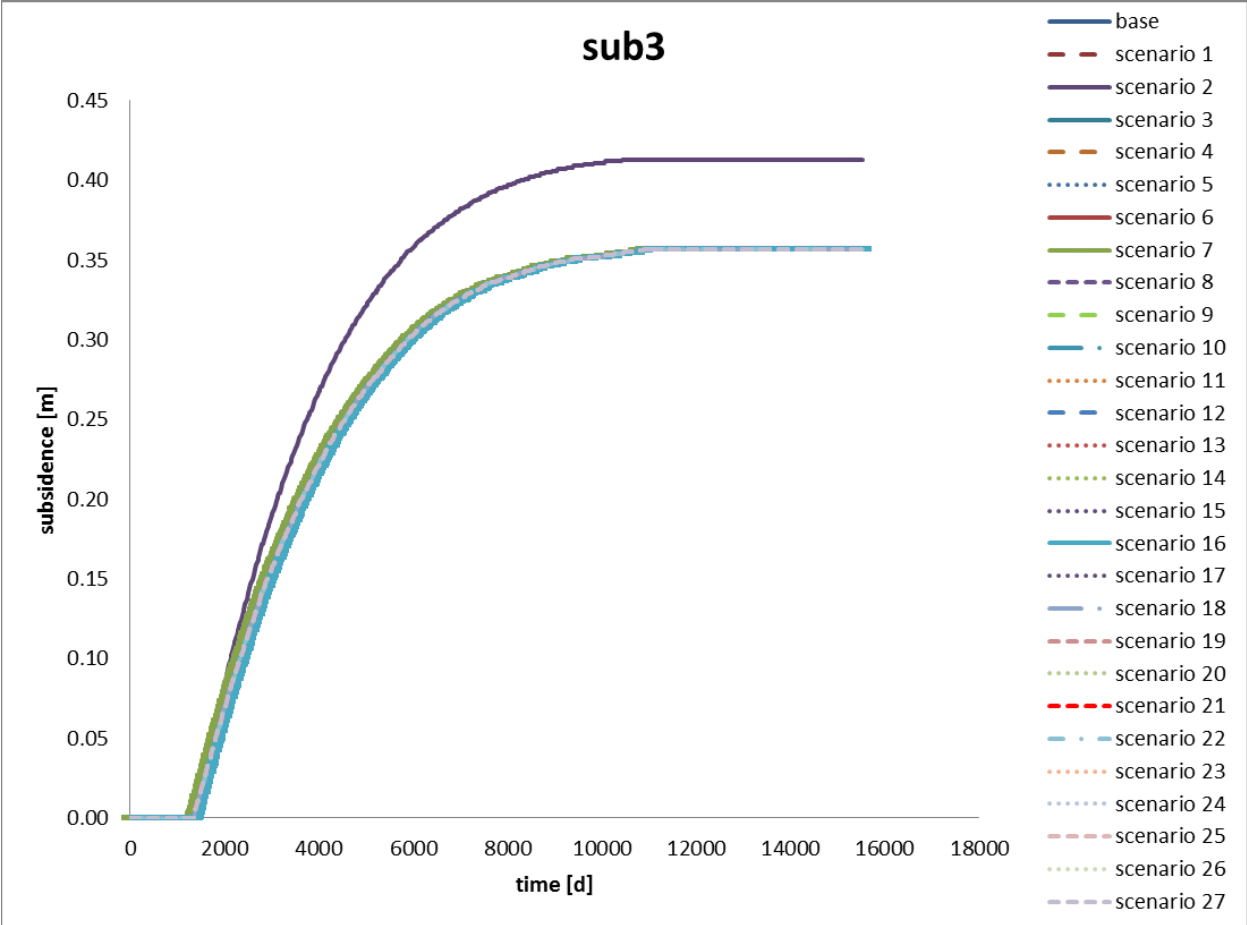
Scenario	Timing	Spacing	Magnitude
1	May/June	North	50,000
2	May/June	Central	50,000
3	May/June	South	50,000
4	July/August	North	50,000
5	July/August	Central	50,000
6	July/August	South	50,000
7	September/October	North	50,000
8	September/October	Central	50,000
9	September/October	South	50,000
10	May/June	North	75,000
11	May/June	Central	75,000
12	May/June	South	75,000
13	July/August	North	75,000
14	July/August	Central	75,000
15	July/August	South	75,000
16	September/October	North	75,000
17	September/October	Central	75,000
18	September/October	South	75,000
19	May/June	North	100,000
20	May/June	Central	100,000
21	May/June	South	100,000
22	July/August	North	100,000
23	July/August	Central	100,000
24	July/August	South	100,000
25	September/October	North	100,000
26	September/October	Central	100,000
27	September/October	South	100,000

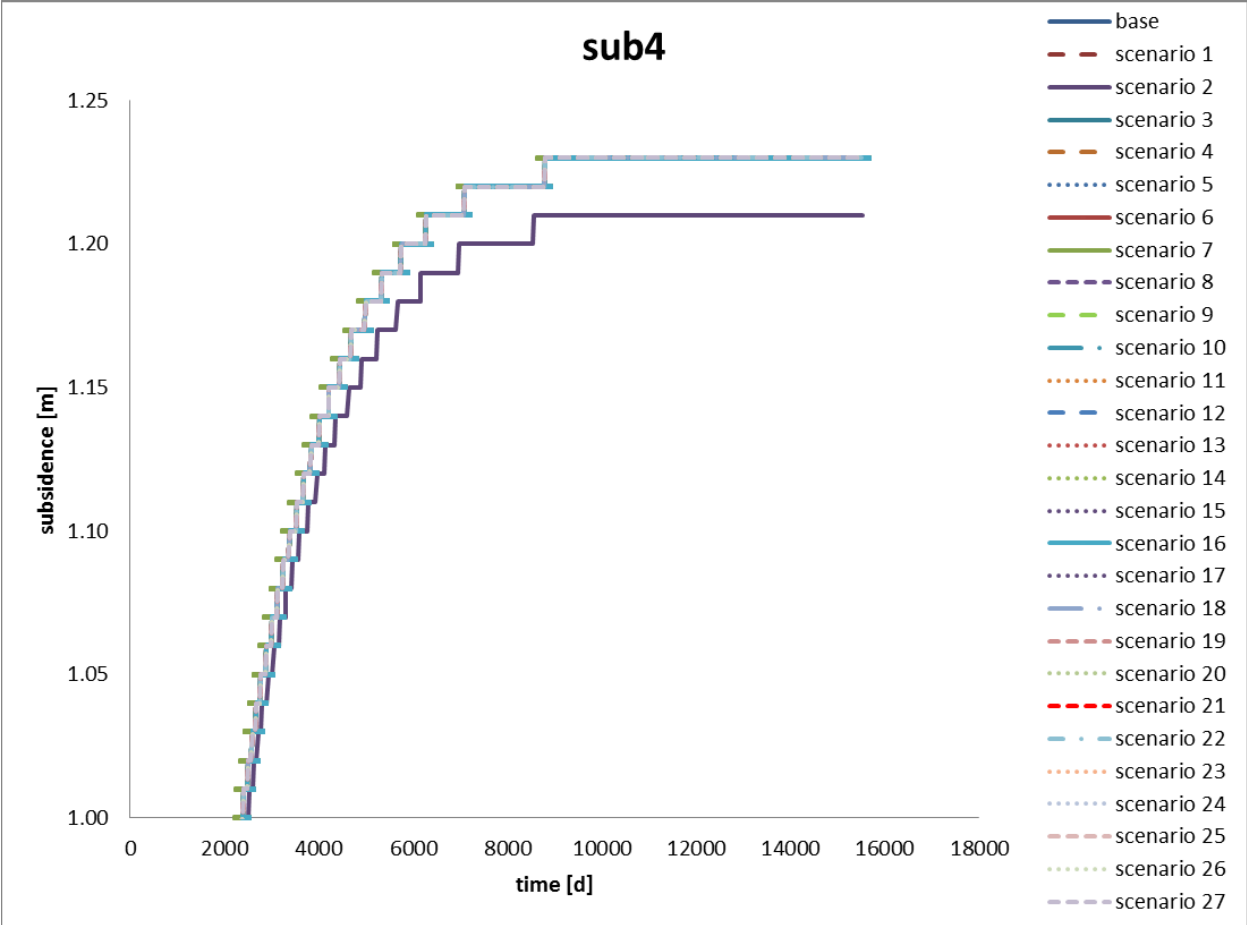
Model Scenario Results

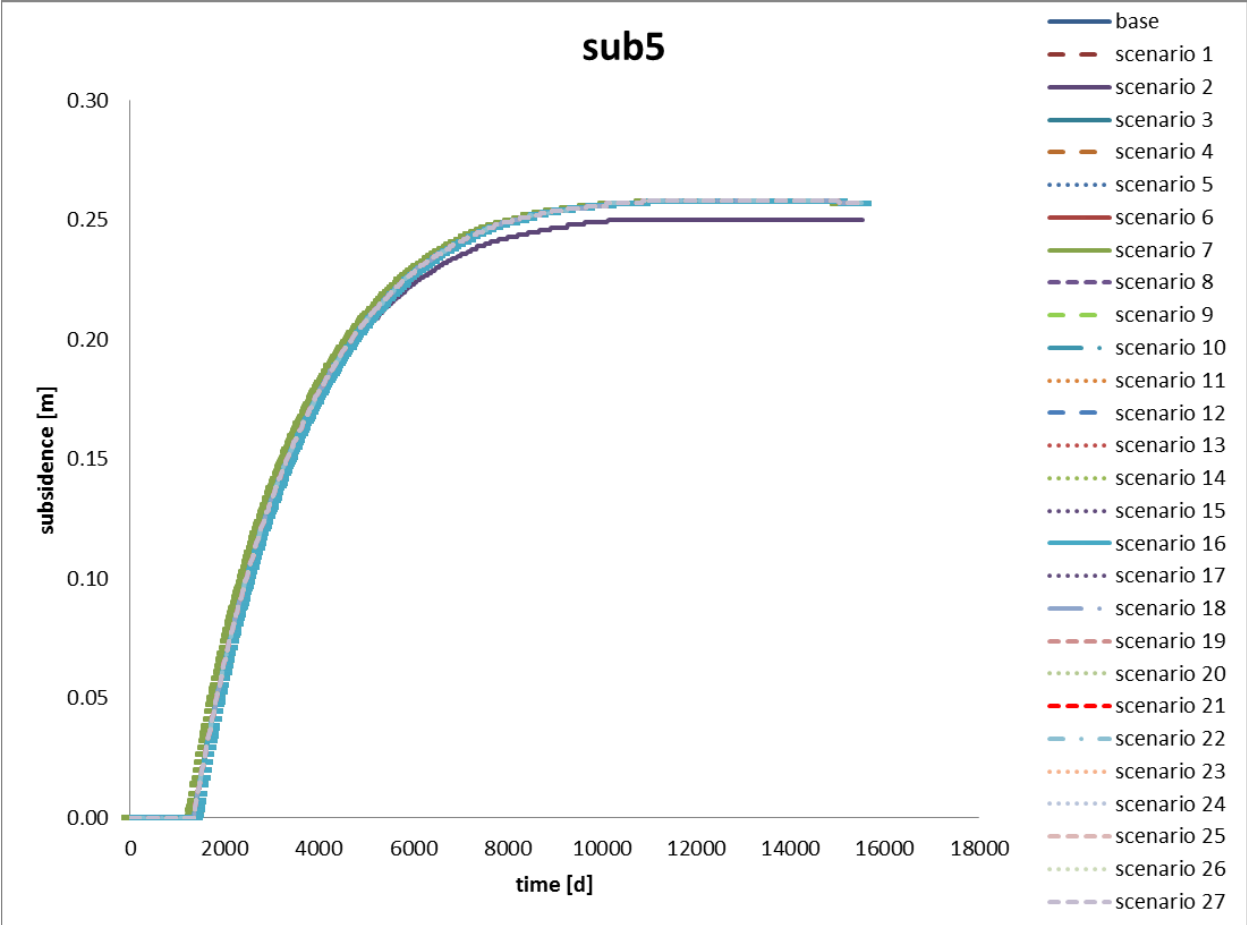
The 27 model scenarios were run and the results analyzed at seven defined subsidence observation locations along the DMC (corresponding to the seven locations used for the transient model calibration in Section 2.2). Figure 7 shows the comprehensive results of these scenarios.

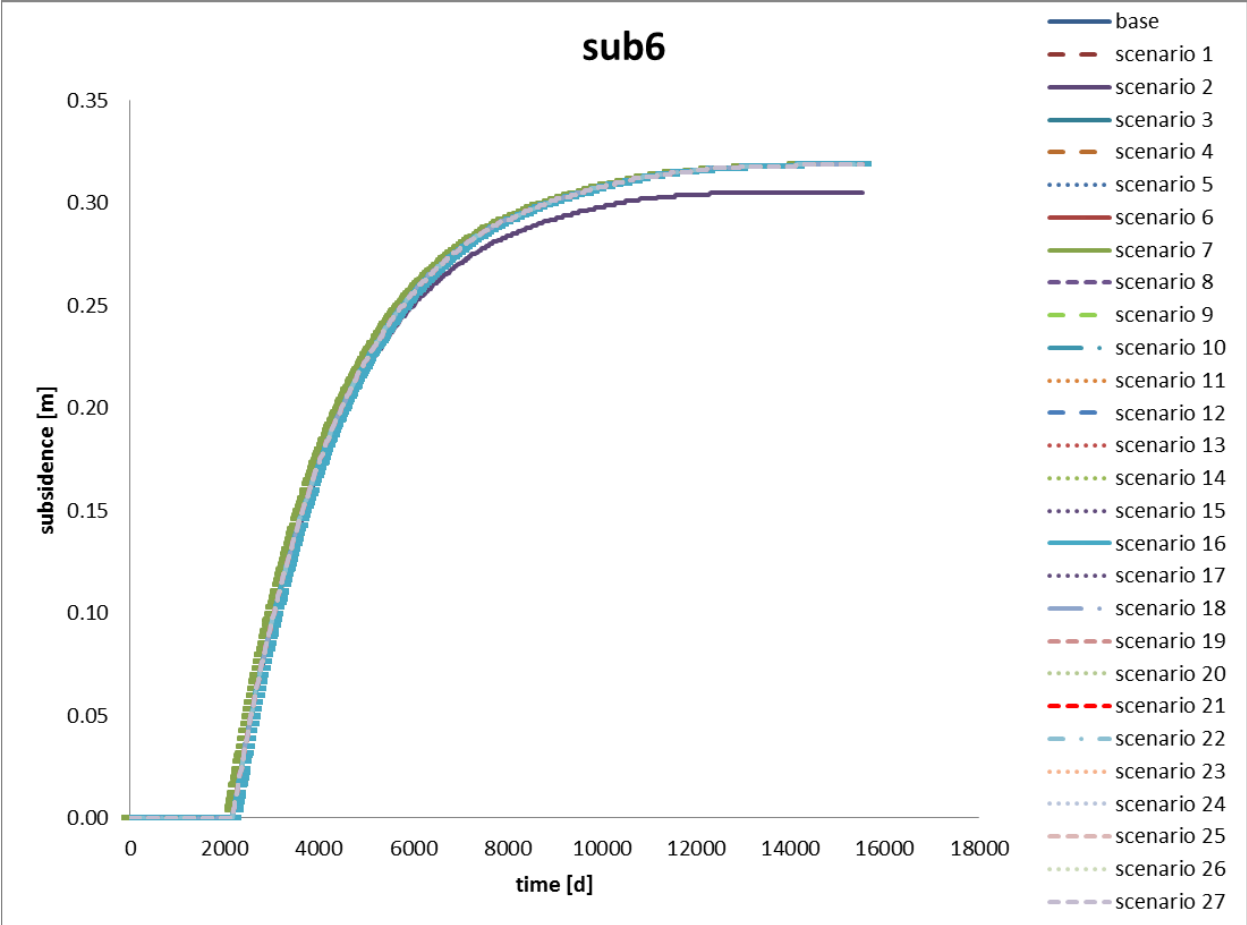












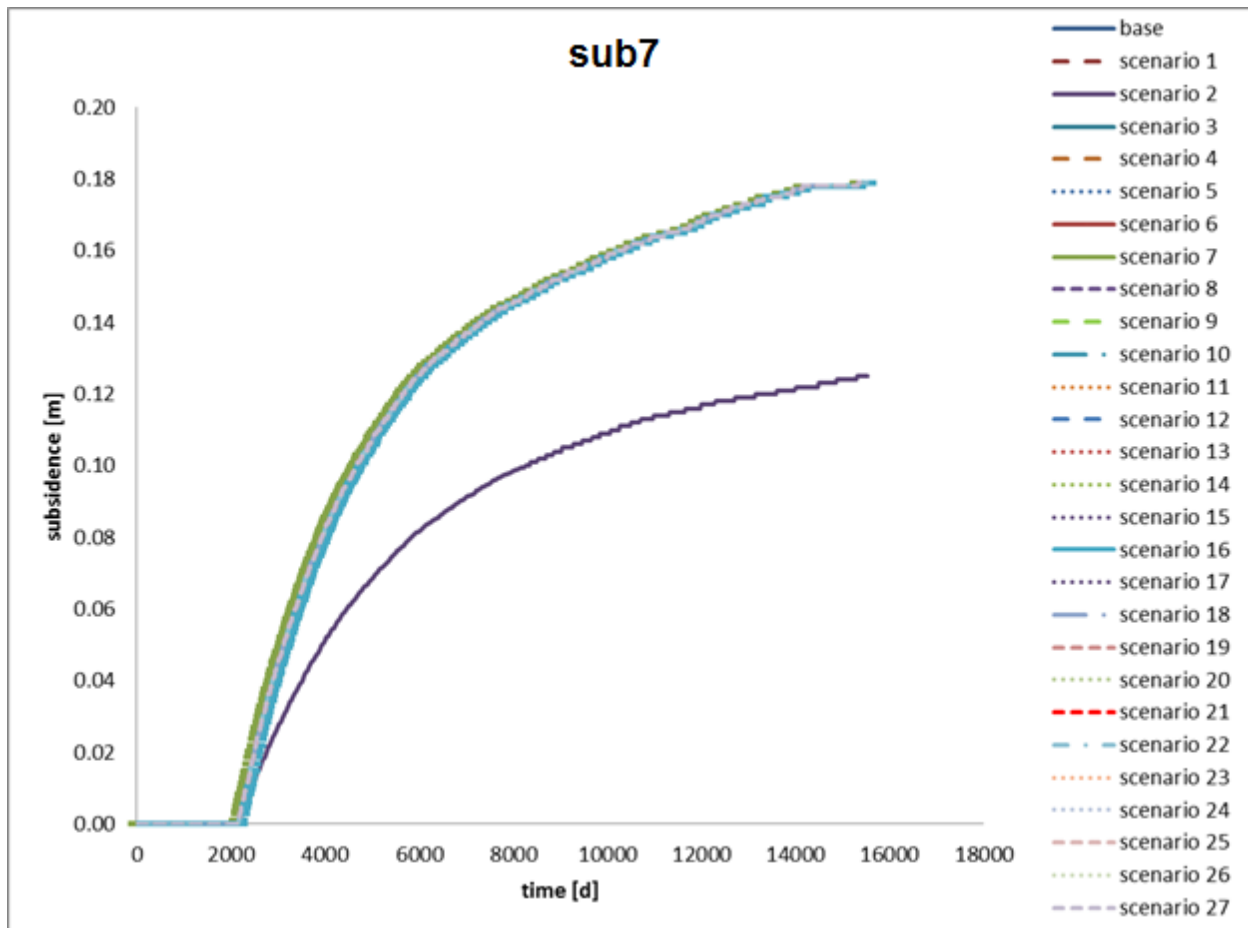


Figure 7. Preliminary Analysis Model Scenario Results. Simulated subsidence for the 27 scenarios compared with the baseline model at the seven subsidence locations along the DMC.

The 27 model scenarios were run and the results analyzed at seven defined subsidence observation locations (corresponding to the seven observation locations used in the transient model calibration). Examination of the model results reveals that the timing factor had negligible impact on the resulting subsidence; for example comparing subsets of scenarios in which the timing factor was the only factor being varied (e.g., scenarios 1, 4, and 7) showed that there was no impact by changing the timing of the pumping. The pumping location factor had a small effect with subsidence increasing as pumping goes from north to south. However, the greatest impact was found with overall pumping magnitude. It is noteworthy, though, that none of the scenarios at the 50,000 acre-ft magnitude resulted in any additional subsidence above the baseline model. Additional subsidence up to 0.5 inches was obtained for the 75,000 acre-ft annual additional pumping scenarios, while additional subsidence up to 1.5 inches was obtained for the 100,000 acre-ft annual additional pumping scenarios.

The 50,000 acre-ft magnitude of additional pumping corresponds to the current limit on Warren Act pumping into the DMC. While this magnitude was not shown to cause any additional subsidence over the baseline amount, an additional scenario was run with the background pumping in HGSSJVM increased by 10% increase and this results in up to 1.5 additional feet of land

subsidence along the DMC (Figure 8). While the Warren Act pumping is not expected to reach this magnitude of increase in pumping, it is reasonable to expect that irrigation districts near the DMC may increase their pumping by such a factor in the face of droughts and surface water delivery reductions. While Reclamation cannot directly regulate or influence such pumping, the newly adopted California Sustainable Groundwater Management Act (SGMA) may eventually impose more direct regulations on pumping such as constraints based on safe yield analyses. Insofar as Reclamation will assist the State in implementation of SGMA and evaluation of groundwater sustainability, consideration of the overall increases in groundwater pumping in response to droughts and other surface water delivery reductions is of relevance to Reclamation.

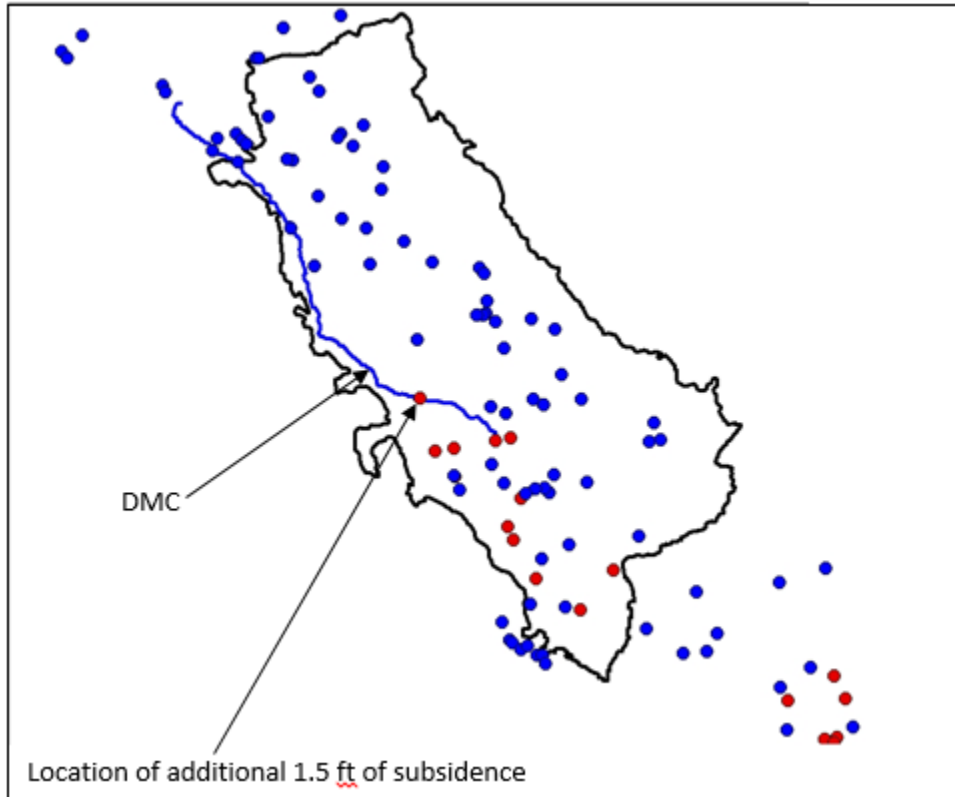


Figure 8. Increased Subsidence from 10% Increase in Background Pumping

Extension of HGSSJVM Through Water Year 2013

Basis for Model Extension

The basis for extending HGSSJVM an additional ten years from its original simulation period (April, 1961 through September, 2003) such that it runs through the 2013 water year is the soon to be released updated version of CVHM (CVHM2). CVHM2 model files were obtained from Jon Traum (USGS). At the time of receiving the CVHM2 model files, USGS was still performing a final calibration of the CVHM2 model parameters; however, the model input data was considered final (Traum, personal communication). In addition to the model files, Jon Traum provided Reclamation with a Python script used for extracting the agricultural well pumping rates produced by the farm package (FMP) within CVHM2.

Data Transfer for Model Extension

In order to extend the HGSSJVM simulation period an additional ten years through water year 2013, it is necessary to obtain time series data for the transient stresses considered by the model. These stresses include both the natural hydrologic processes of precipitation, recharge, and evapotranspiration (ET) as well as the anthropogenic stresses of surface water deliveries, applied irrigation water, and municipal and agricultural groundwater pumping. The CVHM2 model files obtained from Jon Traum were used as the basis for these transient stresses.

The representation of groundwater pumping in the extended HGSSJVM for water years 2004 through 2013 was accomplished by transferring the spatially and temporally distributed pumping values from CVHM2 in a manner similar to that used for the original HGSSJVM simulation period. The transfer of the spatiotemporal groundwater pumping values in CVHM2 into HGSSJVM utilized the same aggregation of CVHM2 representative wells (which in general represent an aggregation of actual, individual wells) into representative wells corresponding to the wells simulated by HGSSJVM. This aggregation methodology was described in Section 2 and yielded the 1023 wells depicted in Figure 4. Having the spatial correspondence between these 1023 wells in HGSSJVM and the wells in CVHM2, the agricultural and municipal pumping rates could be transferred from CVHM2 to HGSSJVM for water years 2004 through 2013. The auxiliary program used to transfer pumping values from CVHM2 to HGSSJVM for water years 1962 through 2003 was modified to account for the additional ten year period and used to transfer the pumping rates for these years. Pumping rates were transferred for the 120 stress periods corresponding to the monthly rates a period of ten years equal to the extended model time series input data.

Like in the original development of HGSSJVM, surface water-groundwater interaction was treated via explicit specifications of infiltration and exfiltration along the ground surface. For the transient model, the CVHM2 spatiotemporal values for precipitation, ET, and surface water deliveries (for irrigation) were transferred to HGSSJVM via the auxiliary parameter transfer program (described in Section 2 above). Spatially, each value represents the sum of the flux in question over one of the ten water balance subregions (regions 8-17) that are coincident to both CVHM2 and HGSSJVM (see, e.g., Figure A8 in Faunt, 2009). Then, a net recharge value was obtained by summing the precipitation and surface irrigation and subtracting the ET for each subregion and each month in the simulation period. For irrigation from groundwater wells, a separate algorithm

was developed so that the irrigation being simulated would be consistent with the agricultural wells as represented in HGSSJVM following the transfer and aggregation of CVHM2 wells. In other words, the process of aggregating and transferring CVHM2 wells into HGSSJVM means that there is not a one-to-one correspondence between CVHM2 and HGSSJVM agricultural wells. Thus, for internal model consistency, rather than taking groundwater well irrigation directly from CVHM2, these irrigation values were determined from the agricultural wells defined in HGSSJVM following the aggregation and transfer process (in a similar manner as described above in **HGSSJVM Model Calibration – Transient Conditions**). Using this approach, the explicit specifications of infiltration and exfiltration along the ground surface needed by HGSSJVM for water years 2004 through 2013 were obtained from CVHM2.

Recalibration of Extended HGSSJVM

To calibrate the extended HGSSJVM, the calibration dataset for the original HGSSJVM was extended with available data at the same locations for the extended period (2004-2013). The calibration data selected consisted of two types: historical groundwater levels and historical compaction (both elastic and the inelastic compaction that results in subsidence). Calibration target locations, as previously described in Section 2, were selected with a focus on the area surrounding the Delta-Mendota Canal (due to the intended initial application of analyzing land subsidence in the DMC area) but also distributed throughout the model domain. In addition to the new data added to the same locations for the new time period, one additional subsidence monitoring location was added: the Oro Loma monitoring location near the southern end of the DMC.

The recalibration of the extended HGSSJVM was accomplished through a manual calibration procedure. First, the thirteen calibration parameters (listed in Table 6) were adjusted both higher and lower by a factor of two (with the other parameters held constant) to assess the sensitivity of results to the augmented calibration dataset. Based on the results of these 26 calibration simulations, four parameters were selected for recalibration: K_{cv} , K_{fv} , S_{sc} , and S_{sf} . An additional 120 manual calibration simulations were run varying these four parameters. Following this procedure, the extended HGSSJVM met the calibration criterion (described in section 2) for the augmented calibration dataset that includes the new subsidence data at Oro Loma. The resulting parameters (with the new values highlighted in bold) are listed in Table 7.

For calibrating the extended HGSSJVM, the calibration period was selected to be the entire simulation period for both the original calibration locations and the Oro Loma site. Figure 8 shows the calibrated (simulated) subsidence values compared to the observed values at the new Oro Loma monitoring location. Visual inspection of the agreement between simulated and measured values at Oro Loma suggests that the extended HGSSJVM is capable of representing the basic relationship between groundwater pumping and land subsidence in the Western San Joaquin Valley generally and specifically for subsidence occurring near the DMC for the more recent period of 2004 through 2013.

Table 6. Calibration parameter values for original HGSSJVM (1961-2003)

<u>Parameter</u>	<u>Initial Guess for PEST</u>
Kch	348 m/day
Kfh	14.93 m/day
ph	0.0011
Kcv	200 m/day
Kfv	14.26 m/day
pv	0.9867
Ssc	$1.0 * 10^{-3} \text{ m}^{-1}$
Ssf	$1.8 * 10^{-1} \text{ m}^{-1}$
Ssi1	$1.0 * 10^{-4} \text{ m}^{-1}$
Ssi2	$1.2 * 10^{-4} \text{ m}^{-1}$
Ssi3	$5.0 * 10^{-4} \text{ m}^{-1}$
Ssi4	$1.1 * 10^{-6} \text{ m}^{-1}$
Sse	$2.0 * 10^{-7} \text{ m}^{-1}$

Table 7. Calibration parameter values for extended HGSSJVM (1961-2013)

<u>Parameter</u>	<u>Initial Guess for PEST</u>
Kch	348 m/day
Kfh	14.93 m/day
ph	0.0011
Kcv	1 m/day
Kfv	$1.0 * 10^{-3} \text{ m/day}$
pv	0.9867
Ssc	$5.0 * 10^{-3} \text{ m}^{-1}$
Ssf	$1.313 * 10^{-1} \text{ m}^{-1}$
Ssi1	$1.0 * 10^{-4} \text{ m}^{-1}$
Ssi2	$1.2 * 10^{-4} \text{ m}^{-1}$
Ssi3	$5.0 * 10^{-4} \text{ m}^{-1}$
Ssi4	$1.1 * 10^{-6} \text{ m}^{-1}$
Sse	$2.0 * 10^{-7} \text{ m}^{-1}$

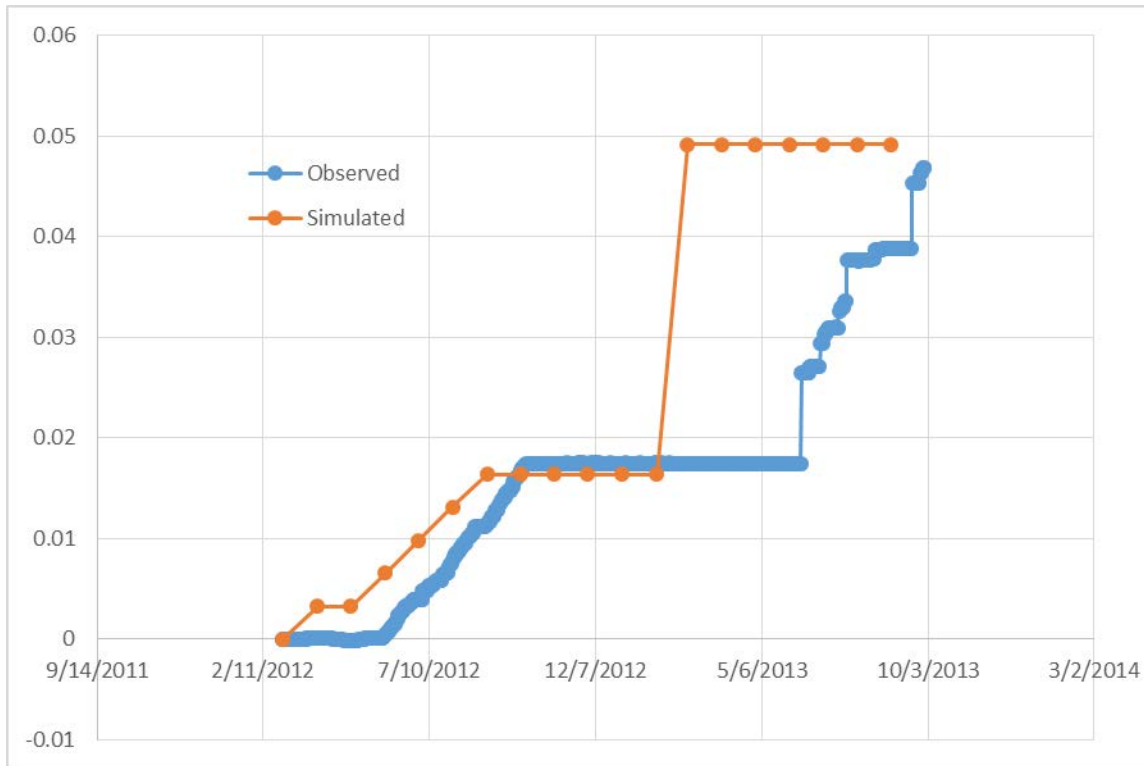


Figure 9. Observed versus simulated subsidence values at Oro Loma

Sensitivity Analysis

A sensitivity analysis was conducted using the final version of HGSSJVM, described in the preceding section, to better understand the groundwater pumping / land subsidence relationship in the Western San Joaquin Valley with a focus on potential impacts to the DMC. With this focus in mind, the sensitivity analysis was designed to examine the impact of parameters that could be modified in the implementation of Warren Act pumping into the DMC. The Warren Act authorizes well owners adjacent to the DMC to pump groundwater into the DMC to augment deliveries to Reclamation contractors. This pumping is authorized for critical, dry, and below normal water year types; Warren Act pumping does not occur in normal and wet water years. The parameters that were considered for this sensitivity analysis were: 1) groundwater pumping magnitude; 2) timing of pumping during the irrigation season; 3) duration of pumping during the irrigation season; 4) spatial location of the Warren Act wells. The existing implementation of the Warren Act pumping program, based on the applicable environmental studies, limits the total annual pumping in critical, dry, and below normal water years to 50,000 acre-ft. The four parameters varied in the sensitivity analysis described in this report were designed to investigate how the land subsidence risk may be affected by: (a) reducing or increasing the limit on total annual pumping; (b) changing the timing of groundwater pumping during the irrigation season; (c) changing the duration of groundwater pumping during the year; and (d) changing the designation of groundwater wells involved in the pumping program among the list of eligible wells.

Scenario Development

The base model for the sensitivity analysis is the calibrated HGSSJVM that was extended to cover the simulation period from water year 1962 through water year 2013. The background pumping in the HGSSJVM is the estimated historical pumping that was derived from the CVHM model using methods described in Faunt (2009). To analyze the effects of the additional groundwater pumping that is authorized in years when the Warren Act provisions are applicable, the following scenarios were formulated. These scenarios represent groundwater pumping that supplements CVP surface water supply during critical, below normal, and dry years.

To investigate the impact of pumping magnitude, three levels of pumping were defined that vary by a factor of two. First, the current limit of 50,000 acre-ft was reduced by a factor of two (i.e., total annual Warren Act pumping = 25,000 acre-ft). Second, Warren Act pumping was set to the current limit of 50,000 acre-ft. Third, Warren Act pumping was increased by a factor of two over the current limit (i.e., total annual Warren Act pumping = 100,000 acre-ft).

To investigate the impact of timing of pumping within the irrigation season, pumping was scheduled to commence at four times during each year: 1) May; 2) June; 3) July; 4) August.

To investigate the impact of pumping duration, the length of time that the pumping is sustained was allowed to vary for periods of time ranging from one to four months. Note that when the pumping duration was varied, the total volume of pumping remained constant. Therefore, variation of the pumping duration parameter had the effect of altering the pumping rate during the month(s) when pumping was active.

To investigate the impact of spatial location of pumping, three sets of wells were defined: 1) Northern; 2) Central; 3) Southern. These definitions correspond to clusters of wells along the three different portions of the DMC. For the selected cluster of wells in a given scenario, the defined pumping was distributed evenly across all wells. These wells were defined based on the actual wells used in the Warren Act program and are listed in Table 8. The Northern cluster of wells corresponds to wells 1-10. The Central cluster of wells corresponds to wells 11-17. The Southern cluster of wells corresponds to wells 18-32.

The water year types (that form the basis for deciding in what years Warren Act pumping is authorized) are listed in Table 9. Although all years of the HGSSJVM simulation period are listed in the table, Warren Act pumping was only considered for the period 1978-2013 with 1981 being the first year when Warren Act conditions were applicable.

The total suite of 90 scenarios defined based on variation of these four parameters is listed in Table 10.

Table 8. Warren Act Wells

Well #	Mile Post	UTM X coordinate (NAD 83)	UTM Y coordinate (NAD 83)
1	21.25L	644349.9638	4167407.775
2	31.6L	655023.4105	4157391.971
3	32.36L	655334.3318	4156206.66
4	33.71L	656925.0903	4155277.978
5	36.01L	658358.7177	4152329.957
6	36.45R	659026.0972	4152134.214
7	36.68R	659355.6468	4151989.103
8	36.8L	659493.9742	4151864.082
9	37.1L	659501.0643	4151380.325
10	37.32L	659661.0835	4151109.58
11	51.66L	668088.2085	4132704.526
12	58.28L	670595.2397	4123351.266
13	78.31L	685266.3272	4100306.488
14	79.13L	686113.8985	4099366.679
15	79.6L	686807.8059	4099022.053
16	80.03L	687311.1926	4098597.875
17	81.08R	688419.2867	4097351.673
18	90.39R	698480.2631	4088439.272
19	90.56L	698723.6426	4088334.895
20	91.36L	699719.4602	4087567.514
21	91.57R	699917.8214	4087292.859
22	91.68R	700062.3515	4087196.388
23	91.77R	700187.4317	4087116.501
24	92.14L	700716.4322	4086908.584
25	92.2R	700815.1792	4086809.498
26	92.72L	701648.9355	4086776.258
27	93.2L	702406.2908	4086871.412
28	93.27R	702522.9621	4086786.726
29	93.27L	702518.5578	4086855.716
30	94.26L	704098.745	4086617.677
31	95.62L	706155.0515	4086103.12
32	99.82L	712384.8291	4084545.758

Table 9. Water Year Types

Year	WY Type
1962	Below Normal
1963	Above Normal
1964	Dry
1965	Wet
1966	Below Normal
1967	Wet
1968	Dry
1969	Wet
1970	Above Normal
1971	Below Normal
1972	Dry
1973	Above Normal
1974	Wet
1975	Wet
1976	Critical
1977	Critical
1978	Wet
1979	Above Normal
1980	Wet
1981	Dry
1982	Wet
1983	Wet
1984	Above Normal
1985	Dry
1986	Wet
1987	Critical
1988	Critical
1989	Critical
1990	Critical
1991	Critical
1992	Critical
1993	Wet
1994	Critical
1995	Wet
1996	Wet
1997	Wet
1998	Wet
1999	Above Normal
2000	Above Normal
2001	Dry

2002	Dry
2003	Below Normal
2004	Dry
2005	Wet
2006	Wet
2007	Critical
2008	Critical
2009	Below Normal
2010	Above Normal
2011	Wet
2012	Dry
2013	Critical

Table 10. Sensitivity Scenarios

Scenario	Number of months	Beginning month	Spatial Location	Magnitude (acre-ft)
1	1	May	Northern	25,000
2	1	June	Northern	25,000
3	1	July	Northern	25,000
4	1	August	Northern	25,000
5	1	May	Central	25,000
6	1	June	Central	25,000
7	1	July	Central	25,000
8	1	August	Central	25,000
9	1	May	Southern	25,000
10	1	June	Southern	25,000
11	1	July	Southern	25,000
12	1	August	Southern	25,000
13	1	May	Northern	50,000
14	1	June	Northern	50,000
15	1	July	Northern	50,000
16	1	August	Northern	50,000
17	1	May	Central	50,000
18	1	June	Central	50,000
19	1	July	Central	50,000
20	1	August	Central	50,000
21	1	May	Central	50,000
22	1	June	Central	50,000
23	1	July	Central	50,000
24	1	August	Central	50,000
25	1	May	Northern	100,000
26	1	June	Northern	100,000

27	1	July	Northern	100,000
28	1	August	Northern	100,000
29	1	May	Central	100,000
30	1	June	Central	100,000
31	1	July	Central	100,000
32	1	August	Central	100,000
33	1	May	Southern	100,000
34	1	June	Southern	100,000
35	1	July	Southern	100,000
36	1	August	Southern	100,000
37	2	May	Northern	25,000
38	2	June	Northern	25,000
39	2	July	Northern	25,000
40	2	May	Central	25,000
41	2	June	Central	25,000
42	2	July	Central	25,000
43	2	May	Southern	25,000
44	2	June	Southern	25,000
45	2	July	Southern	25,000
46	2	May	Northern	50,000
47	2	June	Northern	50,000
48	2	July	Northern	50,000
49	2	May	Central	50,000
50	2	June	Central	50,000
51	2	July	Central	50,000
52	2	May	Southern	50,000
53	2	June	Southern	50,000
54	2	July	Southern	50,000
55	2	May	Northern	100,000
56	2	June	Northern	100,000
57	2	July	Northern	100,000
58	2	May	Central	100,000
59	2	June	Central	100,000
60	2	July	Central	100,000
61	2	May	Southern	100,000
62	2	June	Southern	100,000
63	2	July	Southern	100,000
64	3	May	Northern	25,000
65	3	June	Northern	25,000
66	3	May	Central	25,000
67	3	June	Central	25,000
68	3	May	Southern	25,000
69	3	June	Southern	25,000

70	3	May	Northern	50,000
71	3	June	Northern	50,000
72	3	May	Central	50,000
73	3	June	Central	50,000
74	3	May	Southern	50,000
75	3	June	Southern	50,000
76	3	May	Northern	100,000
77	3	June	Northern	100,000
78	3	May	Central	100,000
79	3	June	Central	100,000
80	3	May	Southern	100,000
81	3	June	Southern	100,000
82	4	May	Northern	25,000
83	4	May	Central	25,000
84	4	May	Southern	25,000
85	4	May	Northern	50,000
86	4	May	Central	50,000
87	4	May	Southern	50,000
88	4	May	Northern	100,000
89	4	May	Central	100,000
90	4	May	Southern	100,000

Sensitivity Analysis Results

To evaluate the results of the 90 sensitivity analysis scenario simulations, 18 observation locations were defined within the model domain running along the length of the DMC. Simulated groundwater level and subsidence values were recorded by SENSAN for use in the sensitivity analysis. The 18 observation locations are listed in Table 11. These locations are shown in relation to the DMC and the Warren Act wells in map contained in Figure 10.

Table 11. Simulation Observation Wells

Observation Well #	UTM X coordinate (NAD 83)	UTM Y coordinate (NAD 83)
1	708927.5	4085273.7
2	665000.0	4150000.0
3	670000.0	4130000.0
4	695000.0	4110000.0
5	705000.0	4090000.0
6	730000.0	4070000.0
7	740000.0	4050000.0
8	675000.0	4150000.0
9	680000.0	4130000.0
10	705000.0	4110000.0
11	715000.0	4090000.0
12	740000.0	4070000.0
13	750000.0	4050000.0
14	715000.0	4079000.0
15	720000.0	4083000.0
16	725000.0	4081000.0
17	728000.0	4073000.0
18	733000.0	4070000.0

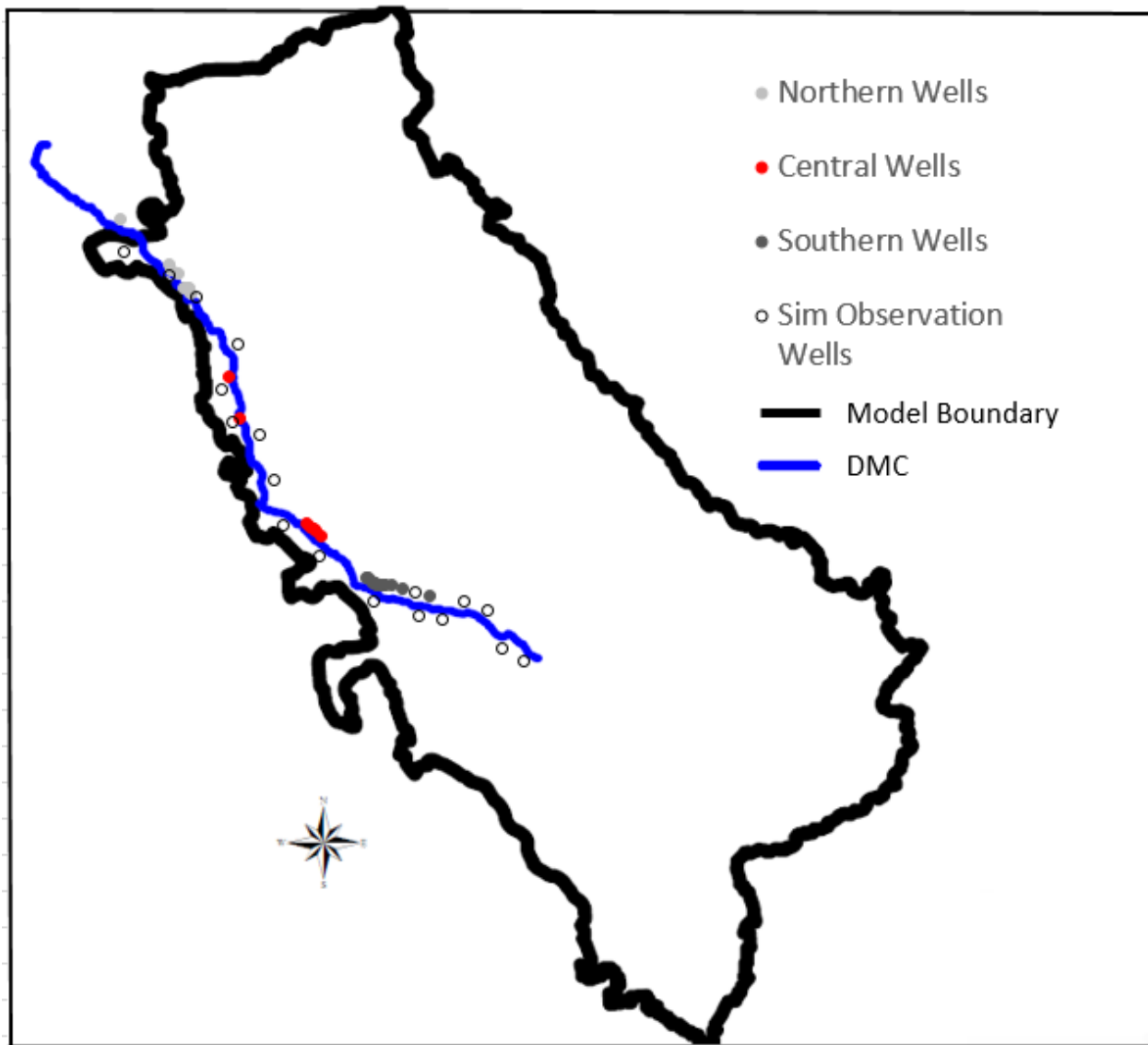


Figure 10. Warren Act Wells and Simulation “Observation” Wells

SENSAN is a model-independent sensitivity analyzer that is part of the PEST suite of model calibration and analysis tools (Doherty, 2002). SENSAN automates the sensitivity analysis process by automating the adjustment of model inputs, running the model, reading the outputs of interest, recording their values, and repeating until all specified parameter adjustments (in this case, corresponding to the scenarios in Table 10) until the sensitivity analysis defined by these parameter adjustments is complete.

SENSAN produces three output files. The first output file gives the output value at selected times for each observation location for each type of output considered (groundwater levels and subsidence values in our case). The second output file gives the relative differences between observation values (note that in SENSAN terminology “observation values” refer to the simulated values of the model output) between different scenarios runs. The third output file gives model

sensitivities with respect to the different parameter variations. The L_2 norm (i.e., square root of the sum of squared differences) is used for the sensitivities.

As a first measure of HGSSJVM sensitivities to the four parameters, results from the first SENSAN output file were examined. These results suggest that HGSSJVM has significant sensitivity to both the total magnitude of Warren Act pumping simulated and the spatial location of the Warren Act pumping wells utilized. However, very little sensitivity was observed for the other two parameters: timing of pumping within the irrigation season and duration of pumping. The sensitivities can be assessed by observing both the scatter of the plotted points and the slope of the regression line. Figures 11-18 display these results for the Oro Loma observation location. The expected relationship between groundwater levels and subsidence (lower groundwater levels correlate with increased subsidence) are exhibited in these results.

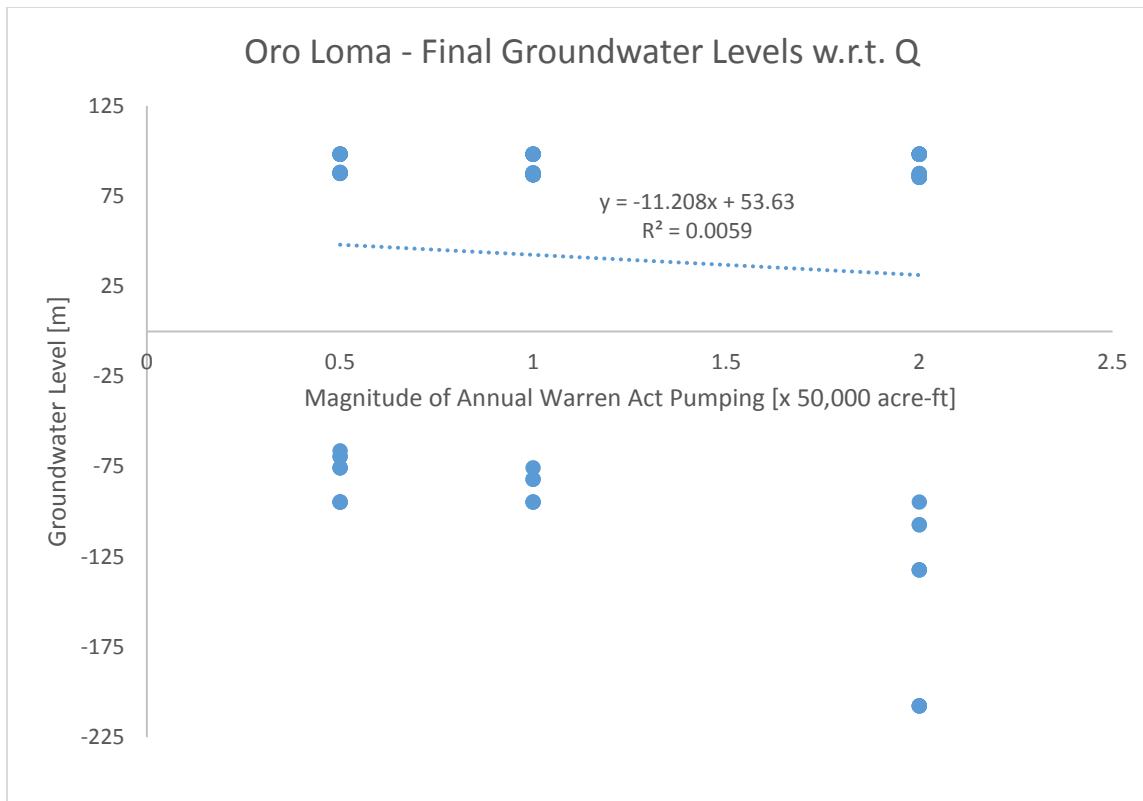


Figure 11. Groundwater Levels at Oro Loma versus Pumping Magnitude. Simulated groundwater levels at the end of the simulation period

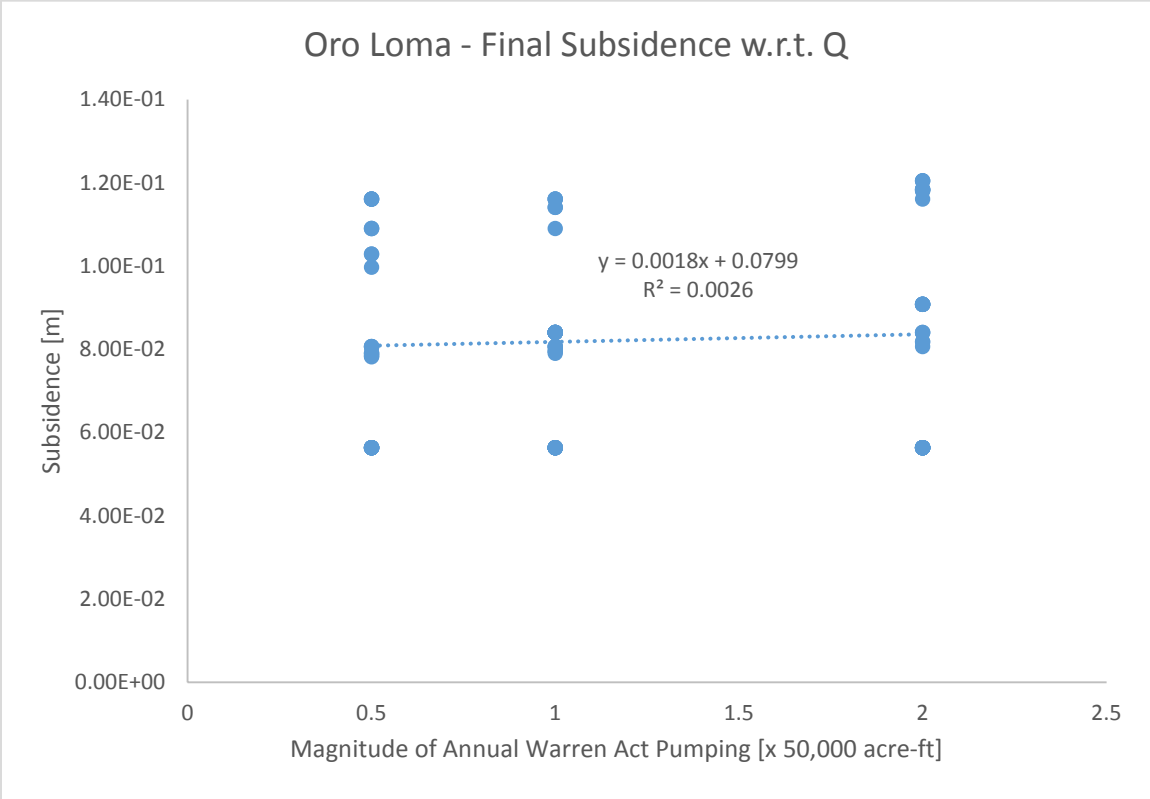


Figure 12. Subsidence values at Oro Loma versus Pumping Magnitude

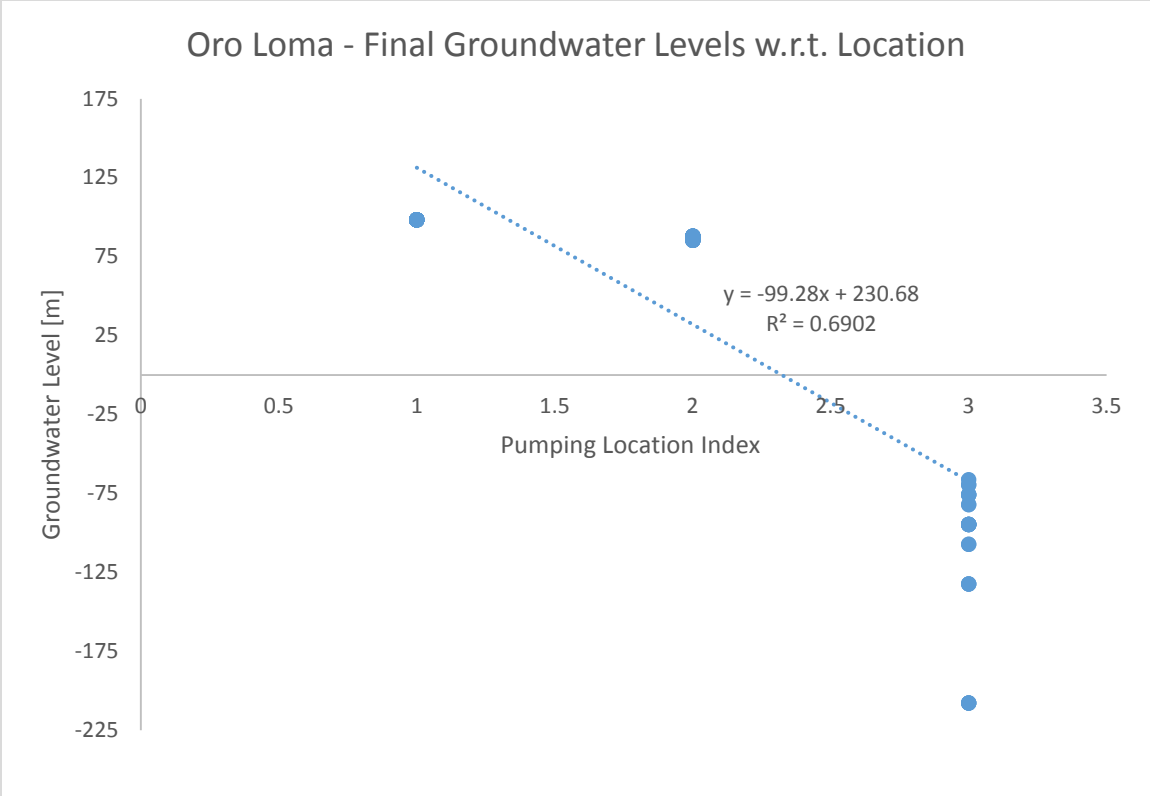


Figure 13. Groundwater Levels at Oro Loma versus Pumping Location

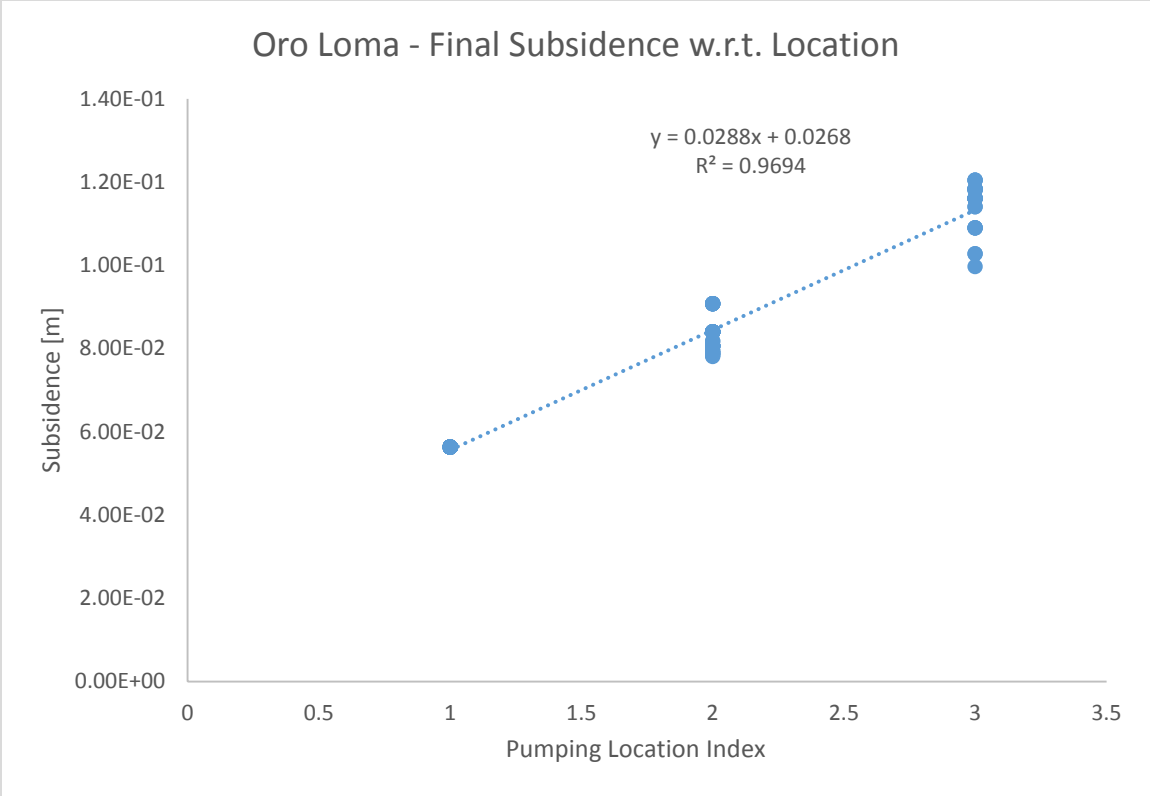


Figure 14. Subsidence values at Oro Loma versus Pumping Location

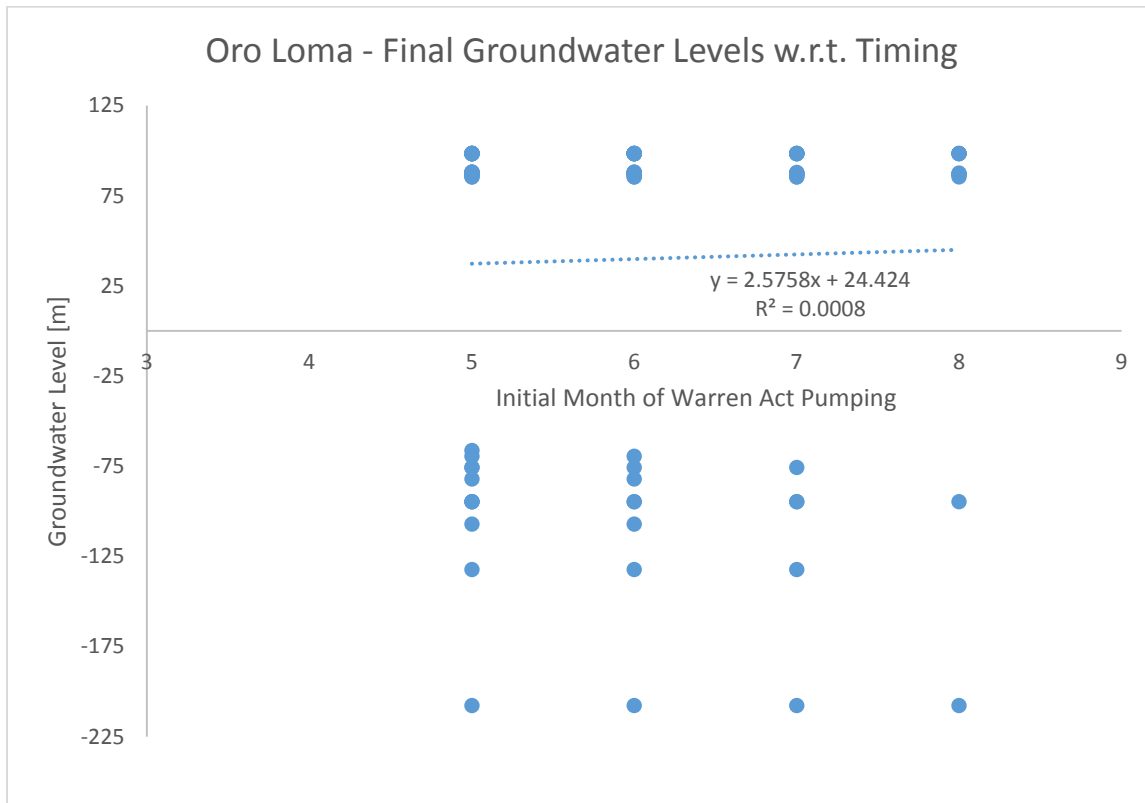


Figure 15. Groundwater Levels at Oro Loma versus Pumping Timing

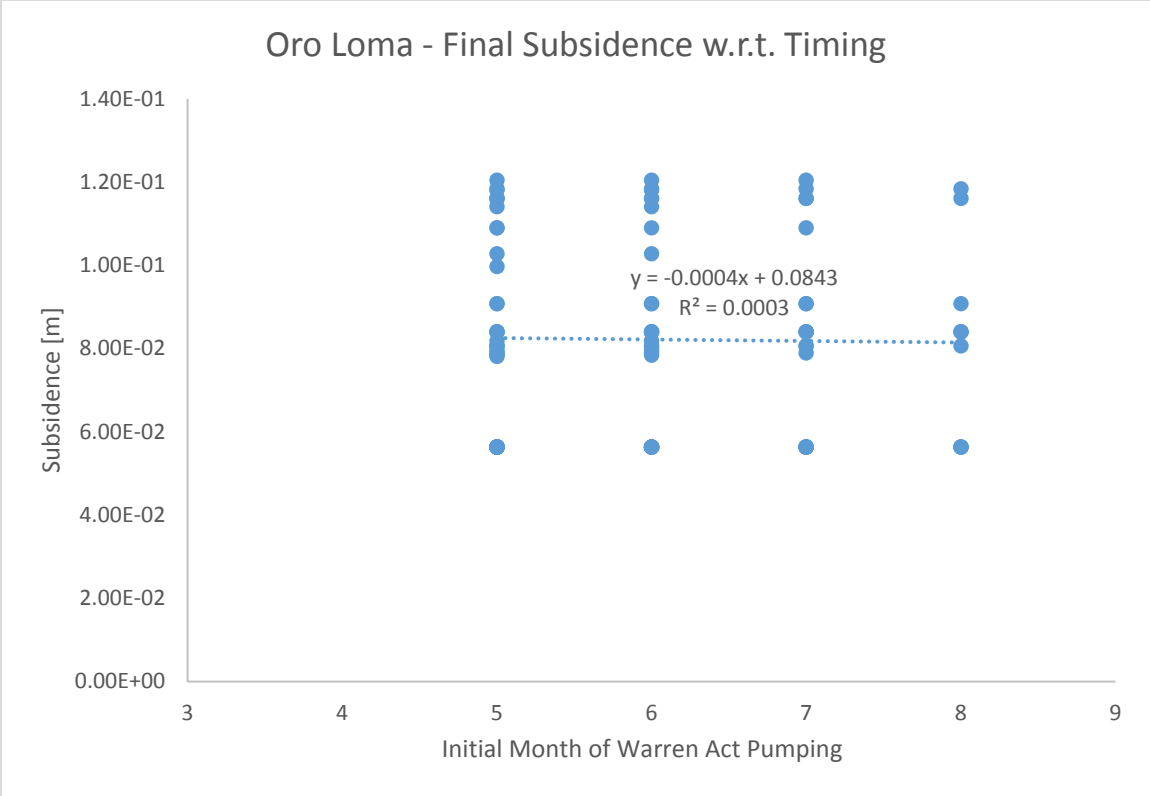


Figure 16. Subsidence values at Oro Loma versus Pumping Timing

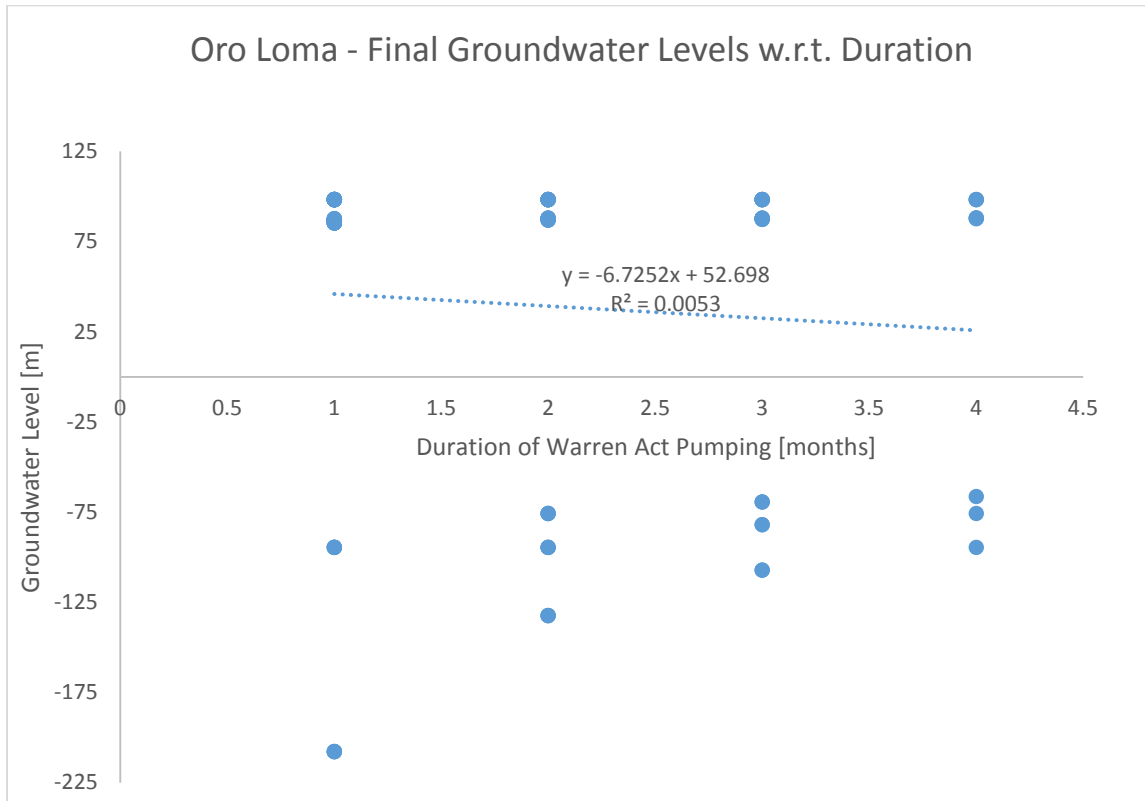


Figure 17. Groundwater Levels at Oro Loma versus Pumping Duration

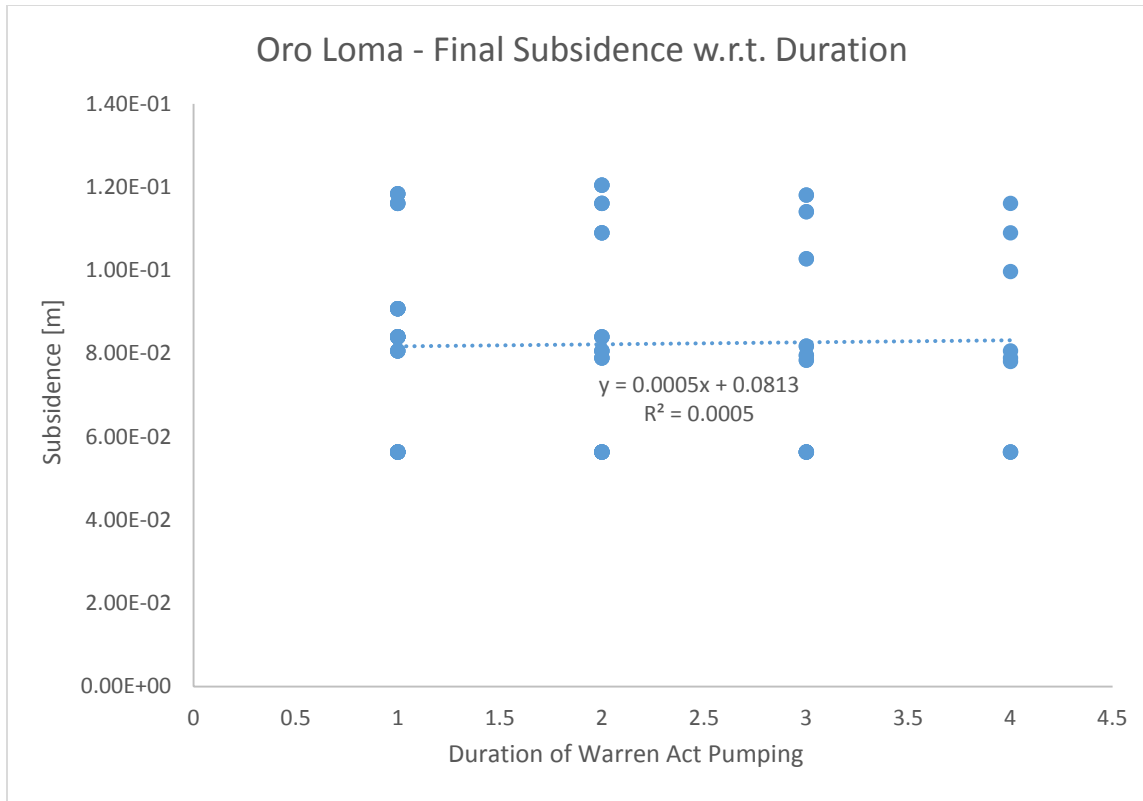


Figure 18. Subsidence values at Oro Loma versus Pumping Duration

Examination of the relative differences between scenario runs reported in the second SENSAN output file yielded similar conclusions about the lesser sensitivity to timing and duration, and the significant sensitivity to magnitude and location. However, by considering the full set of results for the simulated subsidence results at all 18 observation locations defined in Table 11, some differences of the sensitivity results at the different locations did emerge. Table 12 lists the mean slope of sensitivity for each parameter examined in the sensitivity analysis. The mean slopes were calculated by constructing plots similar to the ones in Figures 11, 13, 15, and 17 for each subsidence observation location. Then the slope values were averaged over the 18 locations for each of the four parameters. A positive slope indicates a positive correlation between the parameter of interest and resulting subsidence, while a negative slope indicates an inverse relationship between the parameter of interest and subsidence. As shown in Table 12, the mean slope analysis that takes into account all of the defined observation locations along the length of the DMC has similar results to the analysis focused on the Oro Loma site (observation well #1) in that the greatest sensitivity is with respect to pumping location (also termed spacing) with a mean slope = 0.0061 and the next most sensitive parameter being pumping magnitude with a mean slope of 0.0028. It is important to note, however, that the pumping location (spacing) parameter was the only one of the four parameters to exhibit significant nonlinearity; i.e., not all observation locations were positively correlated with the spacing parameter. The averaged results for spacing yield a positive correlation with increasing subsidence as the pumping locations move south along the canal. However, the correlation was reversed for observation locations 2, 3, 5, 6, and 7 which had slopes of -0.0048, -0.002, -0.0236, -0.0095, and -0.0032 respectively. It is also worth noting that consideration of all observation locations yielded a greater sensitivity with respect to the duration

parameter than the Oro Loma site. This parameter yields a negative correlation with a mean slope of -0.0013. The sign of this correlation suggests that spreading the specified magnitude of Warren Act pumping over a longer period will serve to decrease the subsidence risk.

The sensitivity analysis results are summarized in Table 13. The spatial location parameter having the top sensitivity rank indicates the high importance of well placement in managing subsidence risks due to groundwater withdrawals. The mixed nature of correlation for this parameter reinforces the importance of well locations. As expected, the observation locations closer to the pumping locations tend to exhibit greater simulated subsidence and as the observation location moves farther away from the pumping, the correlation starts to reverse signs. The pumping magnitude parameter is the second most sensitive parameter, and it is consistent in being positively correlated with subsidence across the observation locations. As expected, this suggests that as the magnitude of groundwater withdrawals is increased, subsidence will increase within a given radius of influence. The third most sensitive parameter is pumping duration. The negative correlation of this parameter suggests that for a given magnitude of total groundwater withdrawals for an irrigation season, subsidence can be reduced by distributing the pumping over a greater number of months. The least sensitive parameter is the timing of pumping which suggests that shifting Warren Act pumping to an earlier or later part of the season may have negligible effect.

One additional statistic was calculated to further assess the impact of the overall magnitude of groundwater pumping allowed during an irrigation season under the Warren Act. The mean slope of sensitivity was calculated when the highest pumping level was removed. Thus, this statistic considers only the two cases of pumping at half the currently allowed magnitude (25,000 acre-ft) and the current limit of 50,000 acre-ft. The mean slope calculated based on all sensitivity simulations conducted for these two pumping magnitudes comes out equivalent (0.0028) to the one calculated based on all three magnitude scenarios. In terms of the practical implication of this result, it suggests that the allowable total annual Warren Act pumping magnitude should not be increased over the current limit of 50,000 acre-ft.

Table 12. Mean slope of sensitivity for each sensitivity parameter

Parameter	mean slope
magnitude	0.0028
spacing	0.0061
timing	0.0006
duration	-0.0013

Table 13. Summary of Sensitivity Analysis Results

Parameter	sensitivity rank	correlation
magnitude	2	positive
spacing	1	mixed
timing	4	positive
duration	3	negative

Differential Subsidence

A key factor influencing the risk of subsidence to structures such as the DMC is the phenomenon of differential subsidence where land on one side of the structure experiences subsidence at a different rate from land on the opposite side. In the case of the DMC, differential subsidence creates a torsional stress on the canal that can lead to buckling (an example of which is shown on the cover photo of this report). To evaluate the risk of buckling due to differential subsidence, the sensitivity simulation results were compared for two sets of subsidence observation locations on opposite sides of the canal. The locations chosen for this comparison are given in Table 14. Observation well #1 is paired with observation well #13, and observation well #6 is paired with observation well #7. These pairs of differential subsidence locations are also illustrated in Figure 19.

Table 14. Differential Subsidence Locations

Well #	UTM X coordinate (NAD 83)	UTM Y coordinate (NAD 83)
1	708927.5	4085273.7
13	710000.0	4080000.0
6	669000.0	4122500.0
7	675000.0	4120000.0

To compare the simulated subsidence for each pair of wells listed in Table 14, the mean final subsidence value was computed for all 90 scenarios from the sensitivity analysis. For the well #1/well #13 pair, well #1 had a mean subsidence 8 mm greater than well #13 which corresponds to 10% greater subsidence. For the well #6/well #7 pair, well #6 had a mean subsidence 2 mm greater than well #3 which corresponds to a 31% greater subsidence. The first pair is the more northerly one shown in Figure 18 and the latter is the more southerly one. In the first case the location experiencing greater subsidence is the one to the west of the canal, and in the latter case the location experiencing greater subsidence is the one to the north of the canal. These results suggest that the spatial variability of land subsidence induced by groundwater withdrawals is significant enough to result in damage to the DMC such as buckling. This is consistent with observed damage that has already occurred such as that shown in the cover photo of this report.

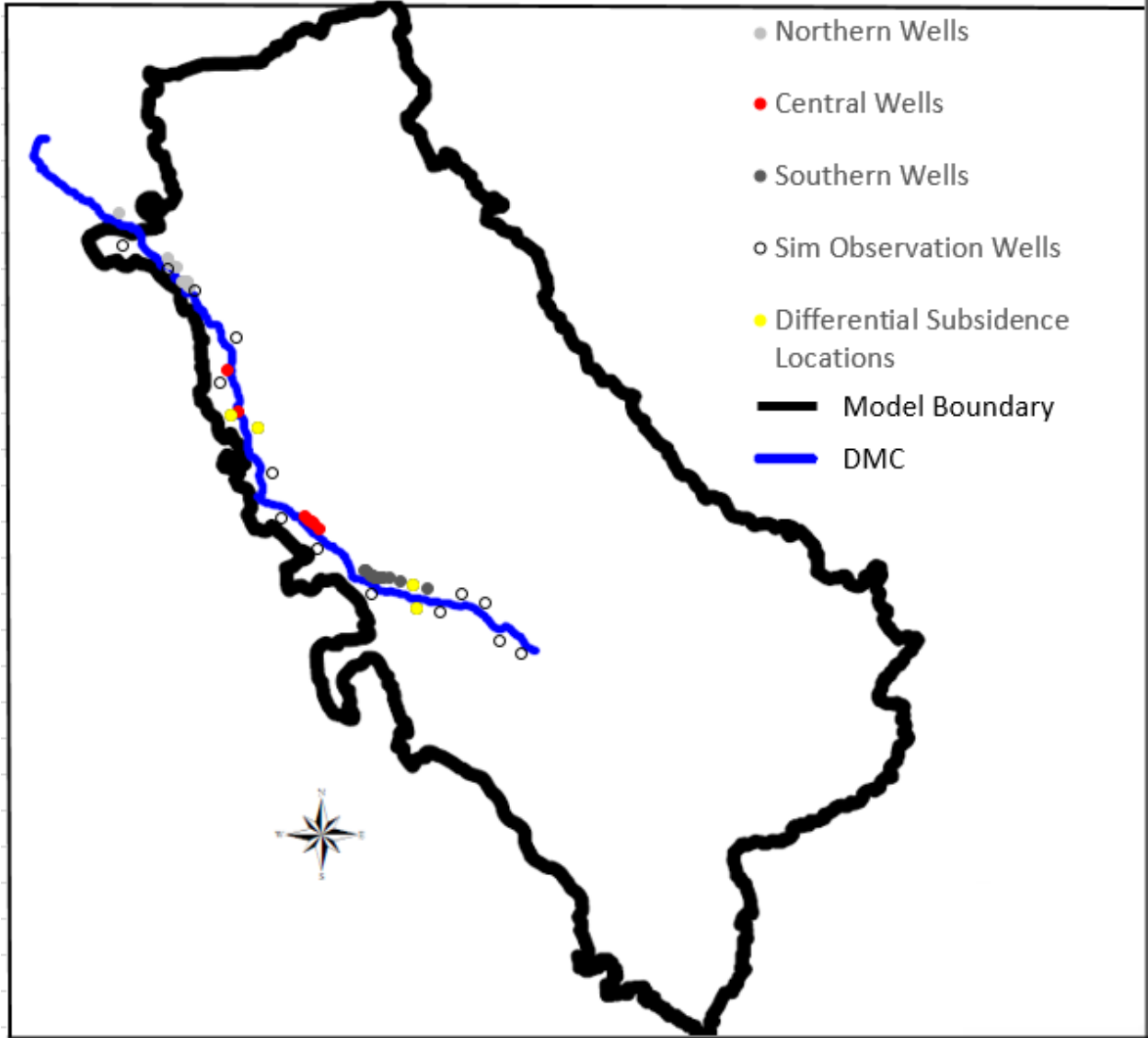


Figure 19. Differential Subsidence Locations

Conclusions & Next Steps

Analysis of the factors impacting the land subsidence risk to the Delta-Mendota Canal (DMC) as a result of groundwater pumping using HGSSJVM suggests several guidelines that could serve to mitigate that risk. Given the sensitivity of land subsidence to the overall magnitude of Warren Act pumping through the range of scenarios simulated by the model that tested both a two-fold reduction and a two-fold increase of the current limit of 50,000 acre-ft/yr - it is recommended that the current groundwater withdrawal limit not be increased. The high degree of sensitivity to the location of groundwater wells used for the withdrawals suggests that undesirable subsidence impacts (particularly as they pertain to the structural integrity of the DMC) can be further mitigated by carefully planning the location of groundwater pumping along the DMC to avoid locations of concern. The results of the sensitivity analysis presented herein also suggest that subsidence impacts can be mitigated by distributing the specified volume of Warren Act groundwater pumping over a longer period of time within a given irrigation season.

Recommended next steps are: (a) to pursue further detailed analyses of the impacts of different groundwater management options on land subsidence in the western SJV using HGSSJVM in coordination with continued field monitoring, such as the recent efforts by Sneed et al. (2013); this would involve interagency cooperation between Reclamation and USGS; (b) in the larger picture of California groundwater management, it is also recommend that Reclamation stay involved in the evolution of the recently enacted Sustainable Groundwater Management Act (SGMA) legislation. This legislation includes subsidence as one of the sustainability factors to be considered by the Groundwater Sustainability Agencies (GSAs) tasked with developing and implementing groundwater sustainability plans for all of the state's groundwater basins. Reclamation is participating on the SGMA Modeling Advisory Committee. This will provide an avenue to coordinate with other modelers such as those from USGS and from California's Department of Water Resources (DWR) working on related model development efforts. For example, future CVHM2 development will emphasize synergistic collaborations that will advance scientific understanding of the relationship between groundwater withdrawals and land subsidence with an aim of creating management strategies that minimize the risk to sensitive receptors such as the DMC in the western SJV. Reclamation will work with colleagues from USGS and DWR to incorporate HGSSJVM into these synergistic collaborations.

References

- Doherty, John, 2002, PEST: Model-Independent Parameter Estimation, Watermark Numerical Computing.
- Faunt, C.C., ed., 2009, Groundwater Availability of the Central Valley Aquifer, California: US Geological Survey Professional Paper 1766, 225 p.
- Hill, M.C., Banta, E.R., Harbaugh, A.W., and Anderman, E.R., 2000, MODFLOW–2000, The U.S Geological Survey modular ground-water model—User guide to the observation, sensitivity, and parameter-estimation processes and three post-processing programs: U.S. Geological Survey Open-File Report 00–184, 209 p.
- Hoffmann, Jörn, Leake, S.A., Galloway, D.L., and Wilson, A.M., 2003, MODFLOW–2000 ground-water model—user guide to the subsidence and aquifer-system compaction (SUB) package: U.S. Geological Survey Open-File Report 03–233, 46 p.
- Huyakron, P.S.; Wu, Y-S.; Park, N.S., 1994, An improved sharp-interface model for assessing NAPL contamination and remediation of groundwater systems, *J. Cont. Hydrol.*, 16: 203-234.
- Ireland, R.L., Poland, J.F., and F.S. Riley, 1984, Land Subsidence in the San Joaquin Valley, California, as of 1980, US Geological Survey Professional Paper 437-I, 93 p.
- Larson, K.J., Basagaoglu, H., and M.A. Mariño, 2001, Prediction of optimal safe ground water yield and land subsidence in the Los Banos-Kettleman City area, California, using a calibrated numerical simulation model, *Journal of Hydrology*, 242: 79-102.
- Leake, S.A. and D.E. Prudic, 1991, Documentation of a computer program to simulate aquifer-system compaction using the modular finite-difference ground water flow model. US Geological Survey Techniques of Water Resources Investigation, Book 6, chap. A2, 68 p.
- McDonald, M.G. and Harbaugh, A.W., 1988, A modular three-dimensional finite-difference ground-water flow model. US Geological Survey Techniques of Water Resources Investigations, Book 6, chap. A1, 586 pp.
- Poland J.F, Lofgren, B.E., Ireland, R.L., and R.G. Pugh, 1975, Land Subsidence in the San Joaquin Valley, California, as of 1972. US Geological Survey Professional Paper 437-H, 78 p.
- Schmid, Wolfgang, Hanson, R.T., Maddock, Thomas, III, Leake, S.A., 2006, User guide for the farm process (FMP1) for the U.S. Geological Survey's modular three-dimensional finite-difference ground-water flow model, MODFLOW-2000: U.S. Geological Survey Techniques and Methods 6-A17, 127 p.
- Sneed, M., Brandt, J. and M. Solt, 2013, Land Subsidence along the Delta-Mendota Canal in the Northern Part of the San Joaquin Valley, California, 2003-2010. US Geological Survey Scientific Investigations Report 2013-5142, 87 p.

Therrien, R., McLaren, R.G., Sudicky, E.A. and Panday, S.M., 2006. HydroGeosphere, a three-dimensional numerical model describing fully-integrated subsurface and overland flow and solute transport. *Université Laval and University of Waterloo, Canada.*

Traum, Jonathan, USGS, 2016, personal communication.

Williamson, A.K.; Prudic, D.E.; Swain, L.A., 1989, Ground-Water Flow in the Central Valley, California: U.S. Geological Survey Professional Paper 1401-D, 127 p.

